© 2018. Published by The Company of Biologists Ltd | Development (2018) 145, dev163535. doi:10.1242/dev.163535

RESEARCH ARTICLE

Nodal signaling has dual roles in fate specification and directed migration during germ layer segregation in zebrafish

Zairan Liu[1,2], Stephanie Woo[3] and Orion D. Weiner[1,2,*]

ABSTRACT

During gastrulation, endodermal cells actively migrate to the interior of the embryo, but the signals that initiate and coordinate this migration are poorly understood. By transplanting ectopically induced endodermal cells far from the normal location of endoderm specification, we identified the inputs that drive internalization without the confounding influences of fate specification and global morphogenic movements. We find that Nodal signaling triggers an autocrine circuit for initiating endodermal internalization. Activation of the Nodal receptor directs endodermal specification through *sox32* and also induces expression of more Nodal ligands. These ligands act in an autocrine fashion to initiate endodermal cell sorting. Our work defines an 'AND' gate consisting of *sox32*-dependent endodermal specification and Nodal ligand reception controlling endodermal cell sorting to the inner layer of the embryo at the onset of gastrulation.

KEY WORDS: Nodal signaling, Ingression, Endoderm, Germ layer segregation, Zebrafish gastrulation

INTRODUCTION

Gastrulation is central to animal development and involves the specification of three different germ layers (endoderm, mesoderm and ectoderm) and their segregation to different locations in the embryo (Wolpert, 1992). In contrast to the mechanisms underlying cell fate specification, the mechanisms used to drive segregation of the three germ layers are much less well understood. In this work, we focus on endodermal cells, which are initially specified on the surface of the embryo but must segregate to the interior, where they give rise to the gut and associated tissues. Endoderm migration is crucial for the formation of the gut tube and digestive tract across the animal kingdom. The in-folding of surface blastoderm cells to form the endoderm is well-documented in a wide range of species (Stern, 2004; Wolpert, 1992). However, it has been experimentally difficult to separate the initiation of migration events from cell fate specification. Thus, the molecular logic of the cell internalization, including which signals trigger this migration and how cell fate and migration are related, still remain unclear.

Several models have been proposed for how the germ layers segregate during embryogenesis. Most prominently, the differential adhesion hypothesis proposed that differences in intercellular adhesion among the different germ layers drives sorting (Steinberg, 1962). However, although differential adhesion and cortex tension have been observed *in vitro*, *in vivo* measurements of tissue surface tension were indistinguishable among the three germ layers. Thus, differential adhesion is unlikely to fully account for the ability of the germ layers to sort in the embryo (Krieg et al., 2008; Maître et al., 2012; Krens et al., 2017).

Previous studies have shown that directed cell migration appears to be the driving force for endoderm segregation *in vivo* for zebrafish (Montero et al., 2005; Krens et al., 2017; Giger and David, 2017). At the onset of zebrafish gastrulation, the blastoderm consists of several thousand cells positioned above the yolk cell. Internalization begins on the dorsal side where inward-moving cells form the hypoblast (mesoderm and endoderm) in contrast to the cells remaining on the outside as epiblast (ectoderm) (Warga and Kimmel, 1990). A germ ring forms at the boundary of hypoblast and epiblast and the embryonic shield is formed on the dorsal side of the margin. Early dye labeling experiments showed that cells relocate to deeper levels within the germ ring by inverting their order relative to the margin as they internalize (Kimmel and Warga, 1987). Initially, an involution model was proposed to describe the population flow as a cellular sheet (Trinkaus, 1984). Later, time-lapse tracking showed that individual cells within the germ ring transiently move out of the epiblast and relocate into the hypoblast (D'Amico and Cooper, 1997; Concha and Adams, 1998). More recent studies have shown that such cells extend protrusions inward and exhibit active directed migration (Montero et al., 2005; Krens et al., 2017; Giger and David, 2017).

Nodal, as a member of the TGFβ superfamily, is essential for germ layer patterning in zebrafish. Nodal ligands are expressed at the margin and yolk syncytial layer (YSL) during the blastula stage, where it forms a morphogen gradient (Chen and Schier, 2001; Dougan et al., 2003). The signaling pathway is activated by Nodal binding to a type II TGFβ receptor, inducing interaction with an EGF-CFC co-receptor, Teratocarcinoma-derived growth factor 1 (Tdgf1; also known as One-eyed-pinhead), and the type I TGFβ receptor Acvr1ba (Weng and Stemple, 2003; Gritsman et al., 1999; Aoki et al., 2002b). Subsequent phosphorylation of the transcription factors Smad2 and Smad3 facilitates the formation, together with Smad4, of a Smad complex that translocates into the nucleus to regulate the expression of target genes (Weng and Stemple, 2003; Jia et al., 2008). One of the key downstream targets is gene encoding Sox32, which plays an essential cell-autonomous role in endoderm formation (Kikuchi et al., 2001).

Compared with endoderm specification, the signals that initiate and direct endoderm migration are not as well understood. From previous studies, it is known that endodermal cells initially undergo random walk migration but switch to convergence movements at mid-gastrulation (Pézeron et al., 2008). Endodermal migration is also regulated by chemokine signaling downstream of the Nodal pathway (Nair and Schilling, 2008; Mizoguchi et al., 2008).

[1]Cardiovascular Research Institute, University of California, San Francisco, San Francisco, CA 94158, USA. [2]Department of Biochemistry and Biophysics, University of California, San Francisco, San Francisco, CA 94158, USA. [3]Department of Molecular Cell Biology, School of Natural Sciences, University of California, Merced, CA 95343, USA.

*Author for correspondence (orion.weiner@ucsf.edu)

O.D.W., 0000-0002-1778-6543

Received 16 January 2018; Accepted 30 July 2018

Development (2018) 145, dev163535. doi:10.1242/dev.163535

We recently demonstrated that Nodal signaling regulates endodermal cell motility and actin dynamics via Rac1 and Prex1 (Woo et al., 2012). However, it is not known whether these migration patterns arise due to endodermal cell fate alone or whether additional cues in their morphogenic field are required.

Here, we utilized an *in vivo* system to study germ layer segregation in zebrafish embryos. In the early zebrafish embryo, an initially mixed mesendodermal population ultimately resolves into distinct mesodermal and endodermal cell layers, but these complex morphogenetic movements occur simultaneously with fate specification (Ho, 1992). To disentangle the endodermal specification program from the migration program, we used a constitutively active version of the Nodal receptor, *acvr1ba**, to predispose cells into an endodermal fate (Renucci et al., 1996; Aoki et al., 2002b; David and Rosa, 2001). By transplanting these ectopically induced endodermal cells into the animal pole of the embryo, we removed them from the endogenous signals that normally orchestrate endodermal development as well as the effects of nearby ingressing cells. We found that these ectopically introduced endodermal cells do not take the normal path of endogenous endoderm migration by internalizing at the germ ring; instead, they radially ingress into the inner layer. Nodal signaling is necessary and sufficient to initiate this process, and the ectopic endodermal cells (but not the surrounding cells) need to receive the Nodal ligand in an autocrine fashion to trigger ingression. Our results suggest that Nodal signaling plays dual roles in specifying endodermal fate and initiating the sorting of these cells to the interior of the embryo. As these migration events are not observed for *in vitro* culture conditions, this *in vivo* approach for endodermal sorting should be a powerful system for continued dissection of the logic of germ layer segregation during gastrulation.

RESULTS

*acvr1ba**-induced endodermal cells ingress into the inner layer of the embryo when placed near the animal pole

To determine the requirements for initiating and directing endoderm migration, we developed a cell transplantation model that allowed us to directly query endodermal sorting while disentangling the endodermal specification program from the migration program. We generated ectopic endodermal cells by expression of the constitutively activated Nodal receptor *acvr1ba**. We then transplanted these cells (Fig. 1A) into the animal pole of a wild-type host embryo, far from the marginal location of endogenous endodermal cells, and determined whether these misplaced ectopic endodermal cells could sort into the correct endodermal layer (Fig. 1B). First, ectopic endoderm production by *acvr1ba** was confirmed by qPCR analysis of *sox17* and *sox32* expression (Fig. S1A), markers for endodermal cell fate (Kikuchi et al., 2001; Shivdasani, 2002). Although Nodal signaling can also induce mesoderm fate (Peyriéras et al., 1998; Aoki et al., 2002b), we found that *acvr1ba** expression upregulated the mesodermal markers *gsc* and *tbxta* (also known as *ntl*) to a lesser extent than *sox17* and *sox32* (Fig. S1B), demonstrating that *acvr1ba**-expressing cells are biased to an endoderm fate. Next, we found that, after transplantation to the animal pole, these ectopically introduced endodermal cells accumulated in endoderm-derived tissue by preferentially migrating to the correct endodermal layer (Fig. 1B-E). When induced endodermal cells were transplanted together with non-endodermal cells (Fig. 1F), these cell types separated into two layers from an originally mixed population (Fig. 1G, Movie 1). Visualizing the migration path of these cells by time-lapse microscopy showed that induced endodermal cells did not move towards the margin and then involute to form endodermal layer (the normal path of endogenous endoderm migration); instead, they radially ingressed into the inner layer (Fig. 1G), consistent with a recent report (Giger and David, 2017). Additional single-cell tracking analysis revealed that the trajectories of transplanted cells did not exhibit random walk or sample both inward and outward directions; instead, the ingression was highly unidirectional (Fig. 1H, Movie 2). These data indicate that endodermal cells produced by *acvr1ba** expression, if placed ectopically, can initiate ingression via highly polarized and unidirectional migration.

Sorting of ectopic endodermal cells requires both Nodal signaling and *sox32*-dependent endoderm specification

We next sought to define the molecular logic of ectopic endodermal cell sorting. In addition to expressing the constitutively activated Acvr1ba* receptor, ectopic endodermal cells can also be produced by overexpression of the transcription factor Sox32, a target of Nodal signaling (Dickmeis et al., 2001; Kikuchi et al., 2001; Sakaguchi et al., 2001). However, previous work suggested that, unlike Acvr1ba* expression, overexpression of *sox32* is not sufficient to drive the sorting process (Kikuchi et al., 2001). We too observed that cells overexpressing *sox32* could preferentially segregate to endoderm-derived tissues when placed near the dorsal margin but not when transplanted to the animal pole (Fig. 2A,B, Fig. S2).

Notably, this means that these two different means of generating endodermal cells (*acvr1ba** versus *sox32*) are not equivalent in their ability to drive internalization movements when transplanted far from the normal endodermal domain (Fig. 2C); only *acvr1ba**-induced endodermal cells are capable of ingression when placed at the animal pole. These data suggest that Nodal signaling initiates endodermal sorting in addition to specifying endodermal fate. *acvr1ba** likely activates additional pathways that are absent when *sox32* is overexpressed, thus allowing cells to sort regardless of the location within the embryo. In contrast, cells overexpressing *sox32* may require extrinsic factors present at the margin to activate these additional 'sorting' pathways, explaining why they can only sort in regions close to the margin (Kikuchi et al., 2001). These observations suggest that the triggering of sorting involves an 'AND' gate consisting of *sox32*-dependent endodermal specification and additional signaling downstream of *acvr1ba** (Fig. 2D).

To confirm the necessity of *sox32*-dependent arm of the putative AND gate, we injected *acvr1ba**-induced endodermal cells with a *sox32* morpholino (MO), which blocks the transcriptional program that initiates endodermal specification (Sakaguchi et al., 2001; Dickmeis et al., 2001) (Fig. S4B). We found that these cells lost the ability to ingress into the inner layer of the embryo after transplantation to the animal pole of a wild-type host (Fig. 2G,H). Single-cell tracking revealed that morpholino against *sox32* (Fig. S5) inhibits the ability of *acvr1ba** cells to migrate to the interior of the embryo. These results suggest that both autocrine production of Nodal ligands and *sox32*-dependent endodermal specification are necessary to trigger ectopic endodermal sorting.

To better understand the differences between these two methods of generating ectopic endoderm, we compared the signaling and transcriptional networks activated by *acvr1ba* and *sox32*. A recent report (Giger and David, 2017) suggested that N-cadherin (Cdh2) expression triggers endoderm ingression. However, we found that both *acvr1ba** and *sox32* overexpression induced *cdh2* expression (Fig. S1C) to similar extents. This suggests that N-cadherin

Development (2018) 145, dev163535. doi:10.1242/dev.163535

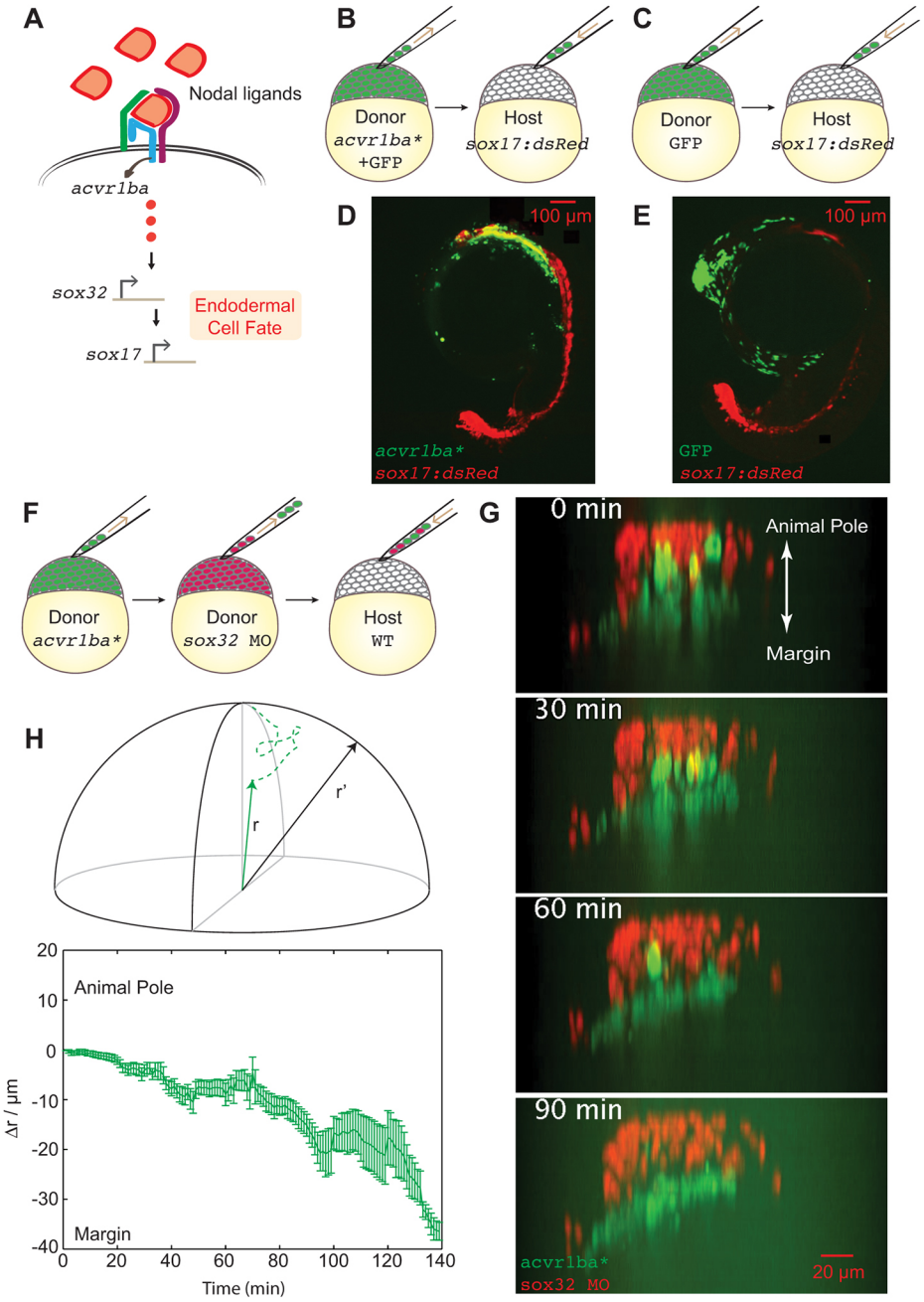

Fig. 1. Constitutively active Nodal receptor (*acvr1ba)-induced ectopic endodermal cells sort into the inner layer of the embryo by ingression.** (A) Schematic depicting Nodal signaling and specification of endodermal cell fate. Nodal ligands activate the Acvr1ba receptor and signal to *sox32*, a transcription factor controlling endodermal specification. (B-E) Schematics of the ectopic endoderm transplant assay (B,C) and representative results (D,E). *acvr1ba**-expressing or control cells were transplanted to the animal pole of *Tg(sox17:dsRed)* host embryos. At 21-somite stage, transplanted *acvr1ba**-expressing cells localized to endoderm-derived tissue, primarily the pharynx (D), whereas control transplanted cells localized to non-endodermal tissue, particularly the head (E). (F) Schematic of the double donor transplant assay. Donor endodermal cells expressing *acvr1ba** (green) were transplanted together with non-endodermal donor cells injected with *sox32* MO (red) to the animal pole of a single wild-type (WT) host. (G) Images from a time-lapse movie of a wild-type host containing both *acvr1ba**-expressing (green) and *sox32* MO-containing (red) donor cells. Time lapse microscopy began immediately after transplantation (0 min). Over time, *sox32* MO donor cells remain in the outer layer of the embryo, whereas *acvr1ba**-expressing donor cells migrate into the inner layer of the embryo. Data were re-sliced and projected onto the *xz* plane, with the animal pole towards the top and the margin towards the bottom. (H) Single-cell tracking analysis of ingression. Top: Cartesian coordinates for transplanted cells were transformed into spherical coordinates. Dashed lines represent cell trajectories. The radial distance, r, was measured as the distance from each cell's position at the end of the time-lapse movie to the center of the embryo (solid lines). r′ was measured as the distance to the host surface for normalization. Bottom: Average relative distance (±s.e.m.) of *acvr1ba**-expressing cells plotted against time. Relative distance for each time point was calculated by measuring the radial distance of *acvr1ba**-expressing cells to the center of the embryo, subtracted by the distance of host cell expanding during gastrulation.

expression alone does not account for the difference of ingression capability between these two types of endodermal cells.

Nodal ligand expression is necessary to trigger the sorting of ectopic endodermal cells

Nodal signaling through *acvr1ba*, but not *sox32* alone, is capable of inducing expression of Nodal ligands *ndr1* and *ndr2* (Chan et al., 2009; Feldman et al., 1998; Dougan et al., 2003). In wild-type embryos, these ligands are expressed at highest levels near the margin, which could explain the observation that *sox32*-induced endodermal cells only sort in this location. In contrast, the autocrine production of Nodal ligands downstream of *acvr1ba** could enable these cells to sort regardless of location in the embryo. To confirm that *ndr1/2* is secreted by *acvr1ba**-expressing cells but not by cells expressing *sox32* alone, we quantified the *ndr1/2* expression profile under all experimental conditions (Fig. S3). When transplanted to wild-type embryos, we saw a 2- to 3-fold increase of *ndr1/2* expression in *acvr1ba**-expressing cells compared with the *sox32*-expressing cells. However, this is likely to be an underestimate of the difference in Nodal ligand expression induced by *acvr1ba** or *sox32* expression because of the presence of maternally deposited *ndr1/2* in the host embryo that can also trigger a Nodal positive-feedback loop. To address this complication, we expressed *acvr1ba** and *sox32* in maternal-zygotic (MZ) *tdgf1* mutant embryos, which lack sufficient Nodal signaling (Gritsman et al., 1999) (Fig. S3B). In this background, we found that *acvr1ba** expression increased *ndr1* expression to a level 25-fold higher than *sox32* expression. Finally, injection of *ndr1/2* mRNA increased the expression of *ndr1/2* in *sox32*-expressing cells to levels similar to those seen in *acvr1ba**-expressing cells (Fig. S3C). Taken together, these

Development (2018) 145, dev163535. doi:10.1242/dev.163535

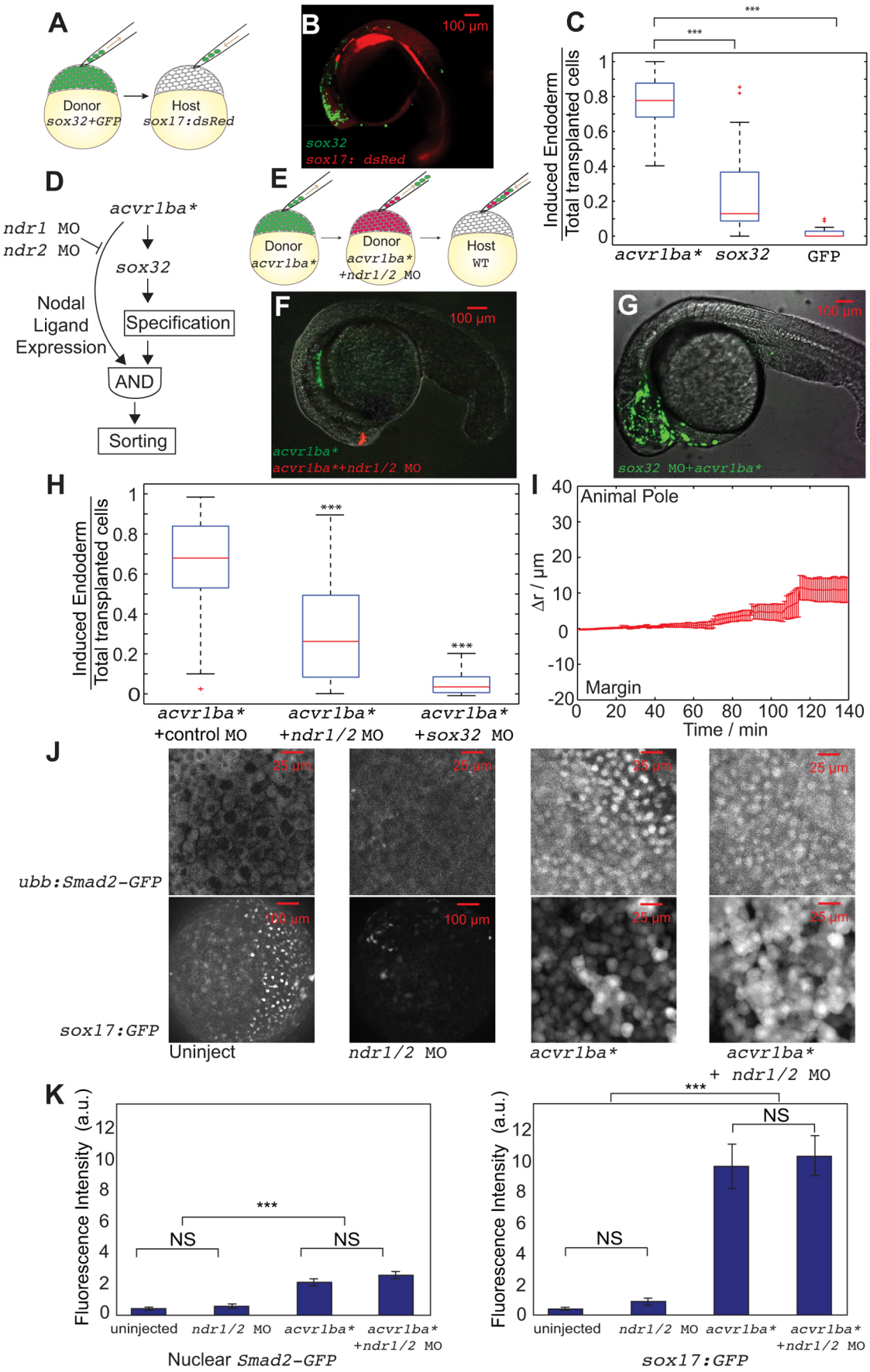

Fig. 2. See next page for legend.

Development (2018) 145, dev163535. doi:10.1242/dev.163535

Fig. 2. Nodal ligand expression is necessary to trigger the sorting of ectopic *acvr1ba-induced endodermal cells.** (A,B) Schematics depicting *sox32*-induced ectopic endoderm transplant assay (A) and representative result (B). *sox32*-overexpressing cells were transplanted to the animal pole of wild-type host embryos. At the 21-somite stage, transplanted *sox32*-overexpressing cells primarily localized to non-endodermal tissues, primarily in the head and skin. (C) Boxplot quantification of endoderm contribution of transplanted cells at 20 hpf, assessed by colocalization with *Tg(sox17:dsRed)* expression. Here and in subsequent figures, for each box, the central mark indicates the median, and the bottom and top edges of the box indicate the 25th and 75th percentiles, respectively. The whiskers extend to the most extreme data points not considered outliers, and the outliers are plotted individually using the '+' symbol. Compared with *acvr1ba**-expressing cells, fewer cells overexpressing *sox32* contributed to endodermal tissues. Data are shown as mean±s.e.m. of three independent transplantation experiments with 26 embryos per condition. ****P*<0.001 (Student's *t*-test). (D) Schematic depicting a potential AND gate for endoderm sorting. Constitutively activate *acvr1ba** upregulates both *sox32* as well as Nodal ligand expression. Only with both inputs do cells successfully sort to the inner layer of the embryo. (E) Schematic of the cell transplantation assay to test the necessity of Nodal ligand expression for cell sorting. Donor cells containing *ndr1* and *ndr2* MOs plus *acvr1ba** mRNA (red) were transplanted together with cells overexpressing *acvr1ba** only (green) into the animal pole of a wild-type (WT) host embryo. (F) Representative images showing the distribution of transplanted cells at the 21-somite stage. Cells expressing *acvr1ba** only (green) localize to endoderm-derived tissue, primarily the pharynx. Cells containing *acvr1ba** along with *ndr1* MO and *ndr2* MO (red) localize to non-endodermal tissue, primarily in the head. Lateral view, anterior to the bottom-left. (G) Representative image showing the distribution of transplanted cells at the 21-somite stage. Cells expressing *acvr1ba** along with *sox32* MO (green) localize to ectoderm-derived tissue, primarily the head. Lateral view, anterior to the bottom-left. (H) Boxplot quantification of endoderm contribution of transplanted cells at 20 hpf. *ndr1* and *ndr2* knockdown as well as *sox32* knockdown reduced the ability of *acvr1ba**-expressing cells to contribute to endodermal tissue. Data are shown as mean±s.e.m. of three independent transplantation experiments with 22 embryos per condition. ****P*<0.001 (Student's *t*-test). (I) Single-cell tracking analysis of ingression of *acvr1ba**-expressing cells with *ndr1* MO and *ndr2* MO. Average relative distance (±s.e.m.) plotted against time. Relative distance was calculated as in Fig. 1H. (J) Nodal signaling levels assessed by *Tg(ubb:Smad2-GFP)* and *Tg(sox17:GFP)*. Top: Smad2-GFP showed no nuclear localization in cells at the animal poles (AP) of uninjected embryos and *ndr1*/*2* morphants. Smad2-GFP showed comparable levels of nuclear localization in *acvr1ba**-injected embryos and *acvr1ba** with *ndr1* and *ndr2* MO-injected embryos. Bottom: Sox17:GFP labels wild-type endodermal cells in the uninjected control embryo but few GFP-positive cells are present in the *ndr1*/*2* morphants. Sox17:GFP shows elevated level of expression in both *acvr1ba**-injected embryos and *acvr1ba** with *ndr1* and *ndr2* MO-injected embryos. Animal pole view. (K) Quantification of Nodal signaling level. Nuclear Smad2-GFP and Sox17:GFP fluorescence levels are quantified. Data are shown as mean ±s.e.m. of three independent embryos. ****P*<0.001 (Student's *t*-test). NS, not significant.

data confirm that *acvrb1a**, but not *sox32*, induces Nodal ligand expression.

Next, we sought to test whether the excess production of Nodal ligands is the driver of ingression. We first examined the necessity of Nodal ligand expression for endodermal sorting by using morpholinos to knockdown *ndr1* and *ndr2* in the *acvr1ba**-induced endodermal cells, which were then transplanted into the animal pole of wild-type embryos (Fig. 2E). We verified the functionality of the morpholinos by demonstrating the inhibition of *sox17* expression (Fig. S4). At 20 hours post-fertilization (hpf), whereas cells expressing *acvr1ba** only preferentially localized to endodermal tissues such as the pharynx, the *acvr1ba** cells with *ndr1* and *ndr2* MO knockdown primarily localized in non-endodermal tissue, particularly in the head region (Fig. 2F,H). Single-cell tracking revealed that the *acvr1ba** cells with *ndr1* and *ndr2* MO remain in the ectoderm and move near the surface of the embryo (Fig. 2I). Notably, the failure to ingress caused by knockdown of *ndr1* and *ndr2* is unlikely to be due to effects on endoderm specification as cells maintained endoderm identity as assessed by *Tg(sox17:GFP)* reporter expression (Fig. 2J,K).

To further test whether *ndr1/2* secretion is necessary for sorting, we analyzed the internalization dynamics of *acvr1ba**- or *sox32*-overexpressing cells in host embryos injected with *ndr1/2* MO. After transplantation into the margin of a *ndr1/2*-depleted host, *acvr1ba**-expressing cells localized to the endoderm-derived tissue (Fig. S6). In contrast to our animal pole transplantation experiments, *sox32*-overexpressing cells transplanted to the margin of *ndr1/2*-depleted hosts were able to contribute to both endoderm and ectoderm-derived tissues, although the extent of endoderm contribution was significantly less compared with *acvr1ba** cells (Fig. S6). Because there are still global morphogenesis movements happening at the margin of the host embryos, it is possible that some transplanted cells are internalized along with their host cell neighbors. Such community effects were previously observed for transplanted MZ *tdgf1* mutant cells that could initially internalize with their wild-type neighbors (Carmany-Rampey and Schier, 2001). This might account for the increased percentage of endoderm contribution for marginally versus animal pole transplanted *sox32*-overexpressing cells.

In zebrafish, the two Nodal ligands Ndr1 and Ndr2 are known for their functional redundancy in inducing mesendoderm fate (Feldman et al., 1998; Erter et al., 1998; Jing et al., 2006). But it is not known whether they behave redundantly to induce ingression. To address this question, we performed transplantation experiments of *acvr1ba**-expressing cells with either *ndr1* MO or *ndr2* MO alone. Our results showed that neither *ndr1* MO or *ndr2* MO abolished the ingression behavior of *acvr1ba**-expressing cells (Fig. S7). These data suggest that these Nodal ligands act redundantly to support the ingression of *acvr1ba**-expressing cells.

Nodal ligand expression is sufficient to drive ingression of *sox32*-induced endodermal cells

Next, we investigated whether addition of Nodal ligands could trigger ectopic endodermal cell sorting in *sox32*-induced endodermal cells, which were not able to ingress into the inner layer when they are transplanted to the animal pole (Fig. 3A). To test this, we injected donor cells with mRNA for both *sox32* and Nodal ligands (*ndr1*, *ndr2*) prior to transplantation into wild-type embryos, using *acvr1ba**-induced endodermal cells as a positive control (Fig. 3B). When examined at the 18-somite stage, *sox32*-injected cells also expressing Nodal ligands accumulated in endoderm-derived tissue significantly better than cells expressing *sox32* alone (Fig. 3D,F,G). These data indicate that the expression of Nodal ligands is sufficient to confer sorting ability in *sox32*-induced endodermal cells.

Can any cell expressing Nodal ligands sort to endodermal tissues, or do cells require both endodermal specification and Nodal ligand expression to support sorting? Because Nodal ligands themselves can drive endodermal fate (Chen and Schier, 2001; David and Rosa, 2001; Dougan et al., 2003), we addressed this question by overexpressing Nodal ligands in conjunction with *sox32* MO (Fig. 3C). We found that Nodal ligands cannot support sorting in the *sox32* MO background (Fig. 3E,G). These data suggest that Nodal ligands can only trigger sorting in conjunction with *sox32*-dependent endodermal specification. Together, our necessity and sufficiency experiments demonstrate that Nodal ligands and *sox32* constitute an 'AND' gate to initiate internalization in the early embryo.

Development (2018) 145, dev163535. doi:10.1242/dev.163535

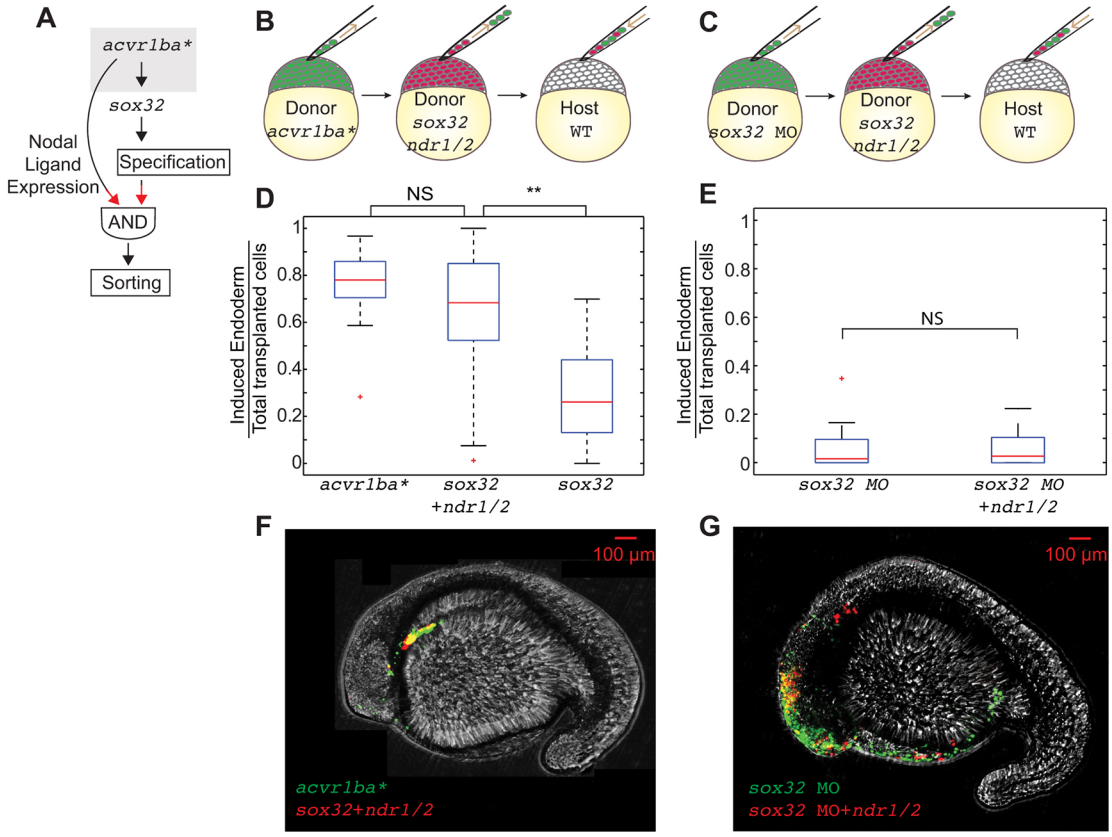

Fig. 3. The combination of Nodal ligand expression and endodermal fate is sufficient to trigger ectopic endodermal cell sorting. (A) Schematic depicting putative AND gate for endoderm sorting. Red arrows demonstrate the experimental perturbation to test the sufficiency of Nodal ligands to induce ingression. (B,C) Schematics of double transplantation assay to test the sufficiency of the AND gate depicted in A for endodermal sorting. Cells overexpressing *acvr1ba** (green) were transplanted together with cells overexpressing *sox32*, *ndr1* and *ndr2* (red) into the animal pole of a wild-type (WT) host embryo (B). Cells containing *sox32* MO only were transplanted together with cells containing *sox32* MO as well as *ndr1* and *ndr2* mRNAs were transplanted into the animal pole of a wild-type host embryo (C). (D) Boxplot quantification of endoderm contribution at 20 hpf of the transplanted cells depicted in B. Cells overexpressing *sox32*, *ndr1* and *ndr2* contributed to endoderm at a similar rate compared with cells overexpressing *acvr1ba**. Data are shown as mean±s.e.m. of three independent transplantation experiments with 18 embryos per condition. $^{**}P<0.01$ (Student's *t*-test). (E) Boxplot quantification of endoderm contribution at 20 hpf of the transplanted cells depicted in C. Neither cells containing *sox32* MO nor cells containing *sox32* MO and overexpressing *ndr1* and *ndr2* contributed to endodermal tissue. In addition, cells expressing *acvr1ba** and *sox32* MO did not contribute to endodermal tissue. Data are shown as mean±s.e.m. of two independent transplantation experiments with 14 embryos per condition. Student's *t*-test. (F) Representative image showing distribution of the transplanted cells depicted in D at the 18-somite stage. *acvr1ba**-expressing cells localize to the endoderm-derived tissue, primarily the pharynx (green). Cells overexpressing *sox32*, *ndr1* and *ndr2* also localize to endoderm-derived tissue, primarily the pharynx (red). Lateral view, anterior to the left. (G) Representative image showing distribution of the transplanted cells depicted in E at the 18-somite stage. Cells expressing *sox32* and Nodal ligands (*ndr1*, *ndr1*) localize to endodermal tissues similar to cells expressing *acvr1ba**. In contrast, *sox32* MO-injected cells (green) and cells injected with *sox32* MO and *ndr1* and *ndr2* mRNAs (red) localize to non-endodermal tissue, primarily in the head and skin. Lateral view, anterior to the left. NS, not significant.

Sorting requires ectopic endodermal cells to receive Nodal signaling in an autocrine circuit

So far, we have shown that Nodal ligand production is necessary and sufficient to trigger the ingression-based cell sorting of ectopic endodermal cells. We next determined which cells are responding to the Nodal ligands to support sorting. The Nodal ligands could either be acting on the same endodermal cells that undergo sorting to form an autocrine circuit or on the surrounding cells in a paracrine circuit, possibly by orchestrating endodermal extrusion by the surrounding ectoderm (Fig. 4A,B). We blocked the autocrine reception of Nodal ligands pharmacologically by applying the Nodal receptor inhibitor SB505124 to *acvr1ba**-expressing cells. We found that 25-50 µM SB505124 inhibited endodermal cell fate specification, even in embryos expressing *acvr1ba**, suggesting that this compound interfered with the signaling circuit upstream of *acvr1ba* (Fig. S8A-C). Following pharmacological Nodal inhibition, *acvr1ba**-expressing cells failed to internalize after being transplanted to the animal pole (Fig. S8D). To inhibit only the autocrine reception of the Nodal ligands while maintaining endodermal cell fate, we used the MZ *tdgf1* mutant to block Nodal signal reception; this mutant lacks the EGF-CFC co-receptor essential for the ability to respond to Nodal ligands (Gritsman et al., 1999). When we transplanted MZ *tdgf1* donor cells expressing *acvr1ba** into wild-type recipient hosts, the donor cells were incapable of ingressing into the inner layer of the host embryo and did not contribute to endoderm-derived tissue at the 18-somite stage (Fig. 4C,F). In contrast, when we injected *acvr1ba** into wild-type donor embryos and transplanted these cells into MZ *tdgf1* mutant host embryos, these transplanted cells still successfully ingressed into the inner layer, indicating that ectopic endodermal cells retained their ability to sort irrespective of the Nodal signaling state of the surrounding cells (Fig. 4D,G). Together, these results suggest that an autocrine circuit of Nodal ligand reception is required to support sorting of ectopic endodermal cells (Fig. 4E). Furthermore, because

Development (2018) 145, dev163535. doi:10.1242/dev.163535

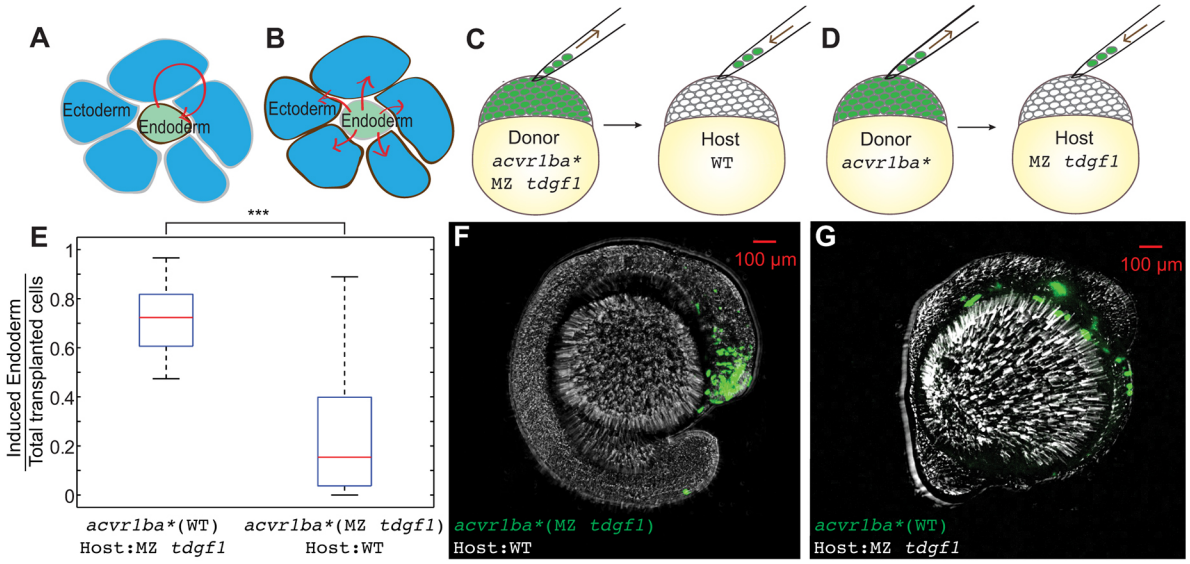

Fig. 4. Nodal ligand reception acts cell-autonomously to support sorting. (A,B) Schematics depicting autonomous (A) versus non-autonomous (B) Nodal ligand reception (red arrows). (C) Schematic depicting single donor transplant assay to test cell-autonomous Nodal signal reception. *acvr1ba**-expressing cells from MZ *tdgf1* donor embryos were transplanted to the animal pole of a wild-type (WT) host embryo. (D) Schematic depicting single donor transplant assay to test non-cell-autonomous Nodal signal reception. *acvr1ba**-expressing cells from wild-type donor embryos were transplanted to the animal pole of a MZ *tdgf1* host embryo. (E) Boxplot quantification of endoderm contribution at the 18-somite stage for all transplanted cells. Wild-type donor cells expressing *acvr1ba** contributed to endodermal tissues whereas *acvr1ba**-expressing cells from MZ *tdgf1* embryos did not. Data are shown as mean±s.e.m. of two independent transplantation experiments, with 14 embryos per condition. ***P<0.001 (Student's *t*-test). (F) Representative image showing distribution of MZ *tdgf1* cells expressing *acvr1ba** in a wild-type host. Donor cells (green) localized to ectoderm-derived tissue, primarily the head. Lateral view, anterior to the right. (G) Representative image showing distribution of wild-type cells expressing *acvr1ba** in a MZ *tdgf1* host. Donor cells (green) localized to endoderm-derived tissue. Lateral view, anterior to the right.

the MZ *tdgf1* mutant host embryos lack endogenous endoderm (Gritsman et al., 1999; David and Rosa, 2001) but still supported ingression of ectopic endodermal cells, these experiments further suggest that signals released by endogenous endodermal cells are not required for ectopic endodermal cell sorting.

It is possible that blocking autocrine Nodal reception, either by pharmacological treatment or loss of *tdgf1*, would also decrease Ndr1/2 production and inhibit ingression. However, given that nuclear accumulation of Smad2 is not significantly different in *acvr1ba**-expressing embryos either with or without *ndr1/2* MO (Fig. 2K), a small decrease in Ndr1/2 production is unlikely to affect the magnitude of Nodal signal to an extent that would impact migration. Therefore, altered levels of Nodal activation do not account for the role of autocrine Ndr1/2 in endodermal internalization. It is more likely that autocrine reception of Nodal ligands may activate other signaling pathways downstream of *acvr1ba** as an input to the 'AND' gate for sorting.

Nodal ligands initiate but do not guide the ingression of endodermal cells

In our transplant experiments, we observed ectopic endodermal cells moving from the outer layer of the embryo radially to the inner layer, but we never observed cells moving in the opposite direction (i.e. extruded from the embryo). A recent study has shown that during normal gastrulation movements, endodermal cells at the margin extend polarized protrusions toward the yolk syncytial layer and appear to internalize by active migration (Giger and David, 2017). Therefore, we investigated whether ectopically placed endodermal cells similarly undergo active, directed migration to enter the interior of the embryo. To visualize actin dynamics in the ectopic endodermal cells during sorting, we expressed GFP-UTRN (Burkel et al., 2007), an actin reporter that we have previously used to analyze endodermal actin dynamics in zebrafish (Woo et al., 2012). We transplanted GFP-UTRN-labeled and *acvr1ba**-induced endodermal cells to the animal pole of wild-type hosts and imaged actin dynamics during ingression. We divided each single transplanted cell into two sectors, one facing towards the interior of the embryo and the other facing towards the embryo surface and then quantified the accumulation of actin in each sector. We observed a significant accumulation of actin in the interior-facing sector of ectopic endodermal cells as well as actin-based protrusions extending towards the interior of the embryo. Control transplanted cells not expressing *acvr1ba** lacked this polarity of actin enrichment and protrusions (Fig. 5A,B). In contrast, *acvr1ba**-expressing cells injected with *ndr1/2* MOs exhibit non-polarized protrusions, suggesting that protrusion generation may be normal but their orientation may be defective in the absence of *ndr1/2* (Fig. S9). Together, these data indicate an asymmetry in protrusion polarization in ectopic endodermal cells but in those with *ndr1/2* knockdown. This indicates that *ndr1* and *ndr2* are necessary to direct the actin-enriched protrusions, consistent with sorting based on active migration.

Which spatial cues are ectopic endodermal cells reading to achieve their directional migration? Such cues are unlikely to arise from the endogenous endodermal cells, as ectopic endoderm can still sort in an MZ *tdgf1* host that lacks endogenous endoderm (Fig. 4E). Might the endogenous Nodal gradient of the host embryo set the direction for ectopic endodermal cell migration? To investigate this hypothesis, we used *ndr1/2* MO to knock down endogenous Nodal ligands in host embryos (Fig. 5C). We transplanted *acvr1ba**-expressing donor cells to the animal pole and found that they maintained their ability to ingress into the inner layer of the embryo (Fig. 5D,G). These data suggest that the endogenous Nodal is not necessary to trigger the sorting behavior. Conversely, we saturated the endogenous Nodal

Development (2018) 145, dev163535. doi:10.1242/dev.163535

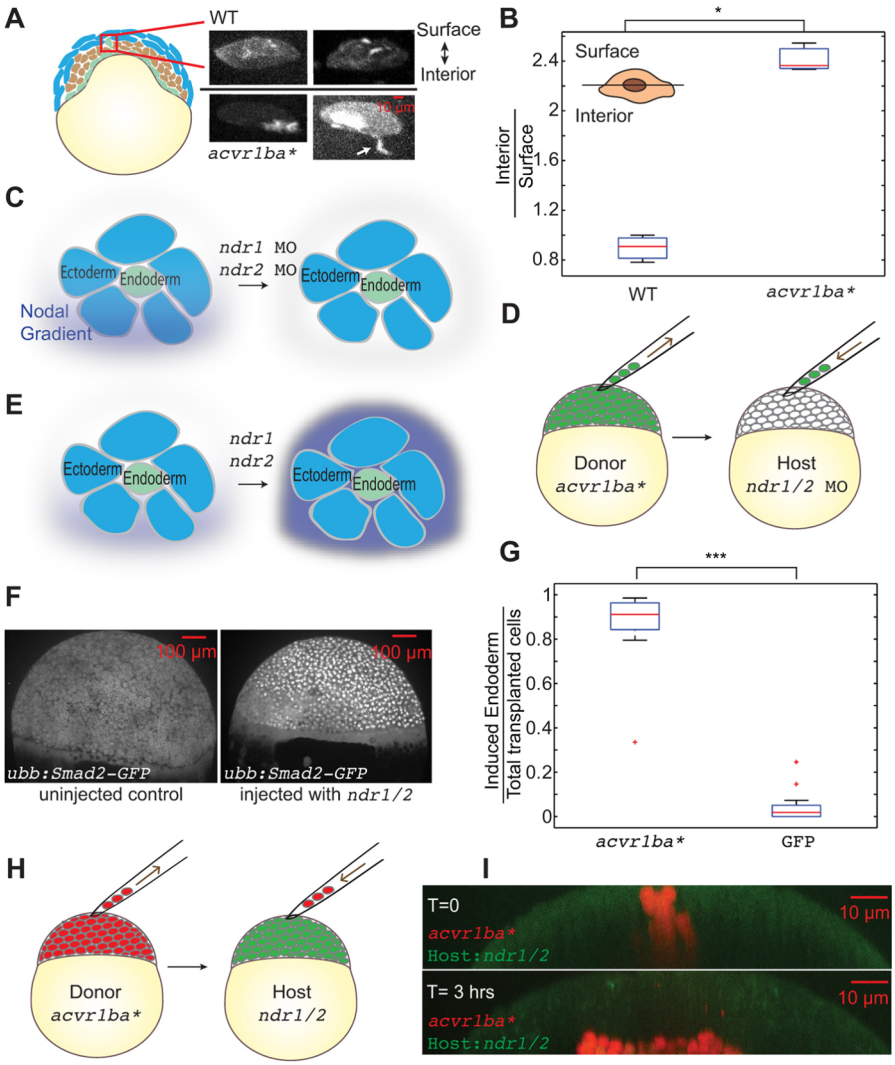

Fig. 5. Nodal ligands initiate but do not guide the ingression of endodermal cells. (A) Actin localization in ectopic endodermal cells. Blue, ectoderm; brown, mesoderm; green, endoderm. Donor embryos were injected with GFP-UTRN mRNA to label actin filaments. Cells overexpressing *acvr1ba** or control cells expressing GFP-UTRN only were transplanted to the animal poles of wild-type host embryos. Actin was enriched on the interior side of *acvr1ba**-expressing cells whereas control cells exhibited uniform actin distribution. Data were re-sliced and projected to the *xz* plane, with the surface of the embryo towards the top and the interior towards the bottom. Arrow shows interior-facing protrusion. (B) Boxplot of the ratio of interior to surface accumulation of actin. *acvr1ba**-expressing cells exhibited significant interior enrichment of actin compared with control cells. Data are shown as mean±s.e.m. of three independent transplantation experiments, with 58 cells per condition. **P*<0.05 (Student's *t*-test). Schematic shows the segmentation of surface versus interior of an endodermal cell. (C,E) Investigation into whether the endogenous Nodal gradient functions as a directional cue for endoderm ingression through knockdown of endogenous Nodal ligands. (C) *ndr1* and *ndr2* MOs were injected into host embryos to remove the endogenous Nodal gradient. (D) Cells expressing *acvr1ba** were transplanted to the animal pole of a Nodal-depleted host. (G) Boxplot quantification of endoderm contribution at 20 hpf for all transplanted cells. Cells overexpressing *acvr1ba** still contributed to endodermal tissues even in the absence of an endogenous Nodal gradient. Data are shown as mean±s.e.m. of two independent transplantation experiments, with 15 embryos per condition. ****P*<0.001 (Student's *t*-test). (E) Saturating the endogenous Nodal gradient to test whether it acts as a directional cue. (F) *Tg(ubb:Smad2-GFP)* shows uniform nuclear translocation in a *ndr1* and *ndr2*-injected embryo, suggesting uniform Nodal signaling. (H) Cells expressing *acvr1ba** were transplanted to the animal pole of a Nodal-saturated host. (I) Representative image showing positions of *acvr1ba** cells (red) immediately and 3 h after transplantation in a Nodal-saturated host.

gradient by overexpressing *ndr1* and *ndr2* ligands in the host embryo (Fig. 5E). As before, the *acvr1ba**-induced endodermal cells retained their ability to ingress into the inner layer (Fig. 5H,I) after transplantation. Together, these data suggest that although autocrine Nodal reception is essential for initiating internalization, neither the endogenous endodermal cells nor the endogenous Nodal ligands spatially direct ingression.

DISCUSSION

In this work, we investigated the molecular signals that initiate the movement of endodermal cells from the surface to the interior of the embryo during zebrafish development. By leveraging the ability of ectopically induced endodermal cells to sort to the endogenous endodermal domain, we dissected the molecular logic of sorting without the confounding influences of fate specification and global morphogenetic movements at the margin. Our work shows that an autocrine circuit of Nodal activated by *acvr1ba** is both necessary and sufficient to trigger internalization of endodermal cells (Figs 2H, 3D and 4E). Neither the endogenous Nodal gradient nor endogenous endodermal cells are required to direct the sorting process. Our work defines an 'AND' gate consisting of *sox32*-dependent endodermal specification and

Development (2018) 145, dev163535. doi:10.1242/dev.163535

Nodal ligand reception that initiates the internalization process (Fig. 3A).

Nodal ligands specify both endodermal cell fate and endodermal sorting

Most of the focus on Nodal signaling during endoderm development has centered around its role in fate specification (Aoki et al., 2002a; Hagos and Dougan, 2007; Dubrulle et al., 2015). Here, we identified an additional role for Nodal as a signaling molecule that regulates endodermal sorting. Endodermal cells that either lack the ability to generate Nodal ligands or to receive Nodal ligands fail to undergo internalization when transplanted to the animal pole (Figs 2H and 4E). Normally, both endoderm specification and Nodal ligand reception occur in the same location in the embryo near the margin, and activation of this 'AND' gate (endodermal specification+Nodal ligand reception) could help specify when and where the internalization process occurs. The requirement for both Nodal ligands and endodermal specification could prevent non-endodermal cells that transiently receive Nodal ligands from internalizing. The autocrine nature of this circuit could help control the timing of internalization, which could be triggered when differentiation has proceeded sufficiently to drive this positive-feedback loop. This positive-feedback loop, in which cells that receive Nodal ligand input release more Nodal ligand, has previously been implicated in the large-scale self-organization of the Nodal field (Chan et al., 2009), and our work demonstrates an additional role for this feedback loop in coordinating endodermal cell sorting. This circuit could also enable the multicellular coordination of internalization. In chick embryos, single-cell ingression can be amplified to induce more of the epiblast to undergo ingression (Voiculescu et al., 2014). Such community effect is Nodal dependent and underlies the formation of primitive streak.

Nodal ligands are received through the Nodal receptor Acvr1ba and its co-receptor Tdgf1 (the zebrafish homolog of TDGF1/Cripto). The constitutively active Nodal receptor Acvr1ba* has frequently been used to investigate the Nodal signaling pathway (Schier and Shen, 2000; Gritsman et al., 1999; Warga and Kane, 2003). Surprisingly, we find that *acvr1ba** requires additional autocrine production and reception of Nodal ligands to support endodermal sorting (Fig. 4). Why might this be? One possibility is that internalization is only triggered above a certain threshold of Nodal signaling. For wild-type cells, this signaling threshold might only be achieved at the margin, where Nodal expression is highest, whereas cells expressing *acvr1ba**, in which Nodal signaling is activated beyond wild-type levels, can reach the thresholds needed for internalization even at positions far from the margin. However, in either case (wild type or *acvr1ba**), these high signaling levels are achieved by a Nodal-induced Nodal expression positive-feedback loop. In *acvr1ba**-induced endodermal cell, Smad2 activation levels are comparable with and without *ndr1/2* knockdown (Fig. 2J,K), suggesting that *acvr1ba** can initiate Nodal signaling independent of Nodal ligands. In future experiments, this model could be tested by perturbing Smad function to varying degrees in the presence of *acvr1ba** and assessing the effects on ingression ability. An alternative explanation for the role of a Nodal autocrine circuit could be activation of *tdgf1*, which may have signaling roles that are independent of *acvr1ba*. This model would be consistent with previous literature showing that *acvr1ba** can only partially rescue *tdgf1* loss of function (Warga and Kane, 2003). In future work, it will be interesting to examine further the differential signaling engaged by *acvr1ba** in the absence and presence of *tdgf1* to identify the *tdgf1*-specific effectors that could participate in endoderm migration.

Directional cues are not limited to Nodal ligands

We dissected the role of Nodal as a trigger for endodermal cell internalization. Through experiments with MZ *tdgf1* as a background for donor and host, we found that ectopic endodermal cells trigger sorting in an autocrine manner. By labeling the actin dynamics, we observed basal enrichment of actin-based protrusions, consistent with other reports suggesting that endodermal cells internalize through active migration (Giger and David, 2017). Previous work in hydra also demonstrated the ability of individual endodermal cells to migrate towards the center of ectodermal aggregates, suggesting that invasion of endodermal cells into ectoderm may represent an ancient morphogenetic behavior (Takaku et al., 2005).

But which spatial cues are these cells reading to migrate towards the interior of the embryo? We ruled out endogenous endodermal cells as an attractive positional cue because *acvr1ba**-expressing cells can ingress in the MZ *tdgf1* background, which lacks endogenous endodermal cells. Moreover, a functioning Nodal gradient does not exist in the MZ *tdgf1* host embryos, suggesting that Nodal itself is not providing positional cues either. This latter point was further demonstrated in our experiments either knocking down the endogenous Nodal gradient or flooding the embryo with uniform Nodal level, both of which failed to block ingression. The intersection of endodermal specification and Nodal ligand reception could unlock the ability of these cells to read other extracellular cues that are polarized from the outside to the inside of the embryo, such as soluble ligands, ECM components and mechanical cues (Piccolo, 2013; Brunet et al., 2013). Apela (also known as Toddler and Elabela) functions as a motogen and enhances the movement of mesodermal and endodermal cells through Apelin receptor signaling, and Nodal is known to activate Apelin receptor expression (Pauli et al., 2014). However, we found that morpholino-directed knockdown of Apelin receptors a and b did not affect the ability of *acvr1ba**-induced cells to ingress into the interior of the embryo (Fig. S10), suggesting that Apela is unlikely to be the spatial cue. Alternatively, the cells could be responding to intrinsic polarity cues, such as an oriented apical-basal polarity followed by apical constriction. Consistent with this idea, *Xenopus* bottle cells and *Caenorhabditis elegans* endodermal progenitor cells have apical-basal polarity and activate apical constriction to initiate gastrulation movements (Nance and Priess, 2002). Clearly, additional work is needed to resolve this question.

Ingression functions as a pattern-refinement mechanism

This work aims to understand the molecular cues that initiate endodermal internalization and germ-layer sorting. In addition to laying the foundation for coordinated cell movement at the primary site of endodermal cell internalization during normal development, single-cell ingression may also function as a backup plan to ensure that endodermal cells that are specified late or otherwise miss initial ingression can still find a path into the inner layer. Given that this sorting behavior is based on an autocrine circuit, endodermal cells can still ingress even if they are no longer adjacent to the margin, and this could increase the precision of the first step of endoderm morphogenesis.

From previous work on zebrafish morphogenesis, it is known that dorsal endodermal cells migrate highly asynchronously, which could lead to challenges in germ layer segregation (Keller et al., 2008). Cell sorting is thought to enable systems with initially noisy fate specification to generate robust final patterns. One extreme example is *Dictyostelium*, in which the initial differentiation decision into prestalk or prespore cell is random, and differential migration is responsible for

Development (2018) 145, dev163535. doi:10.1242/dev.163535

the final pattern (Dormann et al., 2000). Similarly, during neural tube formation in zebrafish, heterogeneous Sonic hedgehog responsivity is sharpened by neural progenitor cells sorting into discrete domains (Xiong et al., 2013). If migration were random, it would be expected to blur the boundaries between different germ layers for cells responding to a source of morphogen such as Nodal. In contrast, by linking directed migration to cell fate specification and signaling, this movement may instead improve the precision of the overall process. By establishing the necessary and sufficient triggers for endodermal sorting *in vivo*, our approach should be useful for continuing to define the logic of endodermal sorting during zebrafish gastrulation.

MATERIALS AND METHODS

Zebrafish strains and embryo maintenance

Zebrafish maintenance was carried out under standard laboratory conditions in the zebrafish facility at Smith Cardiovascular Research Institute. Embryos were grown at 28-31°C in egg water and staged as described previously (Kimmel et al., 1995). The following wild-type, mutant and transgenic lines were used: (wild type) AB/TL; (mutant) *tdgf1*$^{tz57/+}$ (a generous gift from Lilianna Solnica-Krezel's lab in Washington University in St. Louis, MO, USA); (transgenic) *Tg(sox17:GFP)*^{s870}, *Tg(sox17:DsRed)*^{s903}*Tg(h2afva:h2afva-mCherry)*^{tud7}, *Tg(ubb:GFP-Smad2)*^{sfc16}. *Tg(sox17:GFP)*^{s870} and *Tg(sox17:DsRed)*^{s903} (Chung and Stainier, 2008; Mizoguchi et al., 2008) and *Tg(h2afva:h2afva-mCherry)*^{tud7} (Knopf et al., 2011) have been previously described. To construct *Tg(ubb:GFP-Smad2)*^{sfc16}, transgene plasmid mTol2-ubiq:GFP-Smad2 was created by separate PCR amplification of the ubiquitin promoter and GFP ORF and then cloned into pmTol2-ef1a:Venus-Smad2 (gift from Steve Harvey, Wellcome Trust/CR-UK Gurdon Institute and Department of Zoology, The University of Cambridge, Cambridge, UK) cut with *Eco*RV and *Age*I to remove the *ef1a* promoter and Venus ORF. *Tg(ubb:GFP-Smad2)*^{sfc16} was created by injecting 20 pg of the transgene plasmid DNA along with 100 pg of Tol2 transposase mRNA at the one-cell stage. Injected embryos were then sorted by fluorescence on day 0, raised to adulthood, and then screened for founders by outcrossing to wild type. Please refer to Table S2 for a full list of strains used in this study.

Maternal zygotic *tdgf1* mutant generation

To create maternal zygotic *tdgf1* mutants, *tdgf1*$^{tz57/+}$ parents were in-crossed, and all embryos were injected with *tdgf1* mRNA so that homozygous embryos could survive. Genotyping was performed according to established protocols (Hashimoto et al., 2000; Pogoda et al., 2000).

RNA expression construct and morpholino generation

Capped messenger RNA was synthesized using the mMESSAGE mMACHINE kit (Ambion). The following expression plasmids were used in this study: *acvr1ba** in pCS2 (pCS2-acvr1ba*-tBFP), full-length zebrafish *sox32* in pCS2 (pCS2-sox32; Chung and Stainier, 2008), *ndr1* and *ndr2* in pCS2 independently and GFP-UTRN in pCS2. The *sox32* MO was designed to target the translation initiation site and was used at 2 ng (5′-CCTCCTCAGTGTTTATTTCGCTCAT-3′). *ndr1* MO (5′-ATGTCAAATCAAGGTAATAATCCAC-3′) and *ndr2* MO (5′-GCGACTCCCGAGCGTGTGCATGATG-3′) were used at 4 ng. MOs targeting *aplnra* (5′-CGGTGTATTCCGGCGTTGGCTCCAT-3′) and *aplnrb* (5′-CAGAGAAGTTGTTTGTCATGTGCTC-3′) were injected at the one-cell stage at 1 ng or 0.5 ng, respectively. Please refer to Table S2 for a full list of constructs used in this study.

mRNA, morpholino and dye injection

mRNA, morpholino and dye injections were performed with a micromanipulator connected to Picospritzer III. Drop size was regulated by the duration and pressure of the pulse. mRNA of appropriate concentration for different genes was injected into the yolk of the embryo at the one-cell stage. To obtain induced endodermal cells, 0.5 pg *acvr1ba** mRNA or 100 pg *sox32* mRNA were injected into the embryo. To study the effect of Nodal ligands on ingression, 4 pg *ndr1* and *ndr2* mRNA were injected into the embryo. To visualize actin dynamics, 200 pg GFP-UTRN was injected into the embryo. Morpholinos were briefly incubated at 65°C to prevent precipitation and then injected into the yolk before the first cell division. To inhibit the translation of the corresponding genes, 4 ng *ndr1*, 2 ng *ndr1* MO and 2 ng *ndr2* MO (Feldman and Stemple, 2001; Karlen and Rebagliati, 2001), 2 ng *sox32* MO (Sakaguchi et al., 2001), 1 ng *aplnra* MO or 0.5 ng *aplnrb* MO (Scott et al., 2007; Paskaradevan and Scott, 2012; Pauli et al., 2014) were injected into the embryo. Dyes including Dextran-FITC or Dextran-tetra-methyl-rhodamine-dextran (TMR-dextran) or Dextran-Alexa Fluor 680 (Life Technologies) were injected at 1 ng at the one-cell stage to label whole cells and 1 ng Histone H1-Alexa Fluor 488 conjugate (Thermo Fisher Scientific) was injected into the embryo at the one-cell stage to label the nucleus. Please refer to Table S2 for a full list of reagents used in this study.

Real-time quantitative PCR

For Nodal-activated conditions, wild-type embryos were injected at the one-cell stage with 2 pg *acvr1ba** mRNA or *mCherry* mRNA as a control. Expression of *sox17*, a known Nodal target gene, as well as *sox32*, were used to confirm Nodal activation. Expression of *cdh2* was measured under different Nodal-activated conditions. At shield stage, total RNA was extracted using the RNAqueous-Micro Kit, and 1 ng was used for reverse transcription with the SuperScript VILO cDNA Synthesis Kit (Invitrogen). The quantitative PCR reaction mixture contained 2 µl of 10-fold-diluted cDNA, 12.5 µl SYBR green PCR master mix (Applied Biosystems), 714 nM of each primer, and nuclease-free water for a total volume of 25 µl in 48-well plates (Ilumina). Reactions were performed in the Eco Real-Time PCR System (Illumina) as follows: initial activation at 95°C for 10 min followed by 40 cycles of 30 s at 95°C, 30 s at 60°C, and 30 s at 68°C. Once the PCR was completed, a melt-curve analysis was performed to determine reaction specificity. Samples were run in triplicate. The housekeeping gene *ef1a* was used as a reference. Refer to Table S1 for a list of oligonucleotides used in this study.

Transplantation

Donor and host embryos were dechorionated with forceps under a dissection stereomicroscope and transferred into a glass plate with 0.3× Ringer's Buffer. Approximately 25-50 cells were taken from a dechorionated donor embryo(s) at sphere stage (4 hpf) and transplanted into the animal pole of a dechorionated host at the same stage using a beveled borosilicate needle with a 35 µm inner diameter attached to a syringe system. In single donor transplantation experiments, the donor embryo was injected with mRNAs and/or morpholinos described in the main text and wild-type or MZ *tdgf1* embryos were used as hosts. In double donor transplantation experiments, the endoderm donor embryo was injected with 2 pg *acvr1ba** mRNA, control ectoderm donor embryo was injected with 2 ng *sox32* morpholino, and wild-type embryos were used as the host. Dextran dyes were used to differentiate donor versus host cells. H1-Alexa Fluor 488 conjugate was used to label the nucleus for single-cell tracking. After transplantation, embryos were either immediately mounted for microscopy or maintained in 0.3× Ringer's Buffer at 28-31°C for further analysis.

Nodal inhibitor SB505124 treatment

For pharmacological treatment, embryos from one dish were removed at the desired stage and split into glass dishes containing the drug in 5 ml embryo medium, at a density of 25 embryos/dish. For SB505124, the lowest dose that produced the *sqt; cyc* phenotype ranged from 30 to 50 µM, depending on the age of the drug (Hagos and Dougan, 2007). Desired concentration is diluted from 10 mM stock. For transplants, drug treatment is initiated after the transplantation is finished at 4 hpf.

Time-lapse confocal microscopy

Dechorionated embryos, immediately after transplantation, were embedded in 1% low-melting agarose within glass-bottomed Petri dishes, with animal pole mounted towards the glass bottom. For tracking, transplanted embryos were imaged with a 20×/0.75 NA Plan Fluor multi-immersion objective with water as the immersion media. For actin dynamics visualization, a 40×/1.15 NA water immersion objective was used. A 10×/0.45 NA Plan Apo λ objective was used for imaging 24 hpf or 18-somite stage embryos. A high-speed widefield Nikon spinning disk confocal microscope was used for all imaging. This microscope is equipped with an Andor Borealis CSU-W1 unit, an Andor DU-888 EMCCD camera, and a stage-top incubator

Development (2018) 145, dev163535. doi:10.1242/dev.163535

unit from OkoLab. Andor 4-line laser launch (100 mW at 405, 561 and 640 nm; 150 mW at 488 nm) was used for excitation. Micro-Manager Open Source Microscopy Software Version 2.0 Beta was used to control the microscope. Image stacks of 70-150 µm with 1-2 µm (1 µm for time lapse and 2 µm for end-point scanning) *z* stack were recorded in continuous mode, resulting in an image sampling rate of 2-4 min. Embryos were kept at 28.5°C throughout imaging.

Image processing

Tracking with Gaussian Mixture Models (TGMM) software for automated large-scale segmentation and tracking of fluorescently labeled cell nuclei from the Keller Lab was adapted for single-cell tracking of the transplanted cells (Amat et al., 2014). Time-lapse datasets with *z*-stacks were rendered into 3D tracks and filtered by track length. A sphere was used for modeling the zebrafish embryo, and Cartesian coordinates were transformed into spherical coordinates to determine the radial distance traveled by the transplanted cells.

Quantification and statistical analysis

Quantification of the percentage of transplanted cells that localized to endodermal versus non-endodermal domains was performed by analyzing images with Fiji. *z*-stack images were converted to maximum intensity projections and thresholded by Renyi entropy. Particles were analyzed with Fiji and size of regions of interest were measured. For image re-slicing, *z*-stack images were re-sliced to achieve 1×1×1 voxel size, then converted to maximum intensity projections to generate an *xz* projection. Statistical data analyses were performed using Student's *t*-test in Matlab.

Acknowledgements

We thank Steve Harvey for plasmid (pmTol2-ef1a: Venus-Smad2), Lilianna Solnica-Krezel for providing the *tdgf1* zebrafish line, Philipp Keller for providing guidance on TGMM tracking software and Alba Diz-Muñoz for feedback on the manuscript. We are grateful to Jeremy Reiter, Wallace Marshall, Sophie Dumont and the Weiner group for fruitful discussions, and the zebrafish facility at CVRI and NIC at UCSF for assistance.

Competing interests

The authors declare no competing or financial interests.

Author contributions

Conceptualization: Z.L., O.D.W.; Methodology: Z.L., S.W.; Formal analysis: Z.L.; Writing - original draft: Z.L.; Writing - review & editing: S.W., O.D.W.; Funding acquisition: Z.L., S.W., O.D.W.

Funding

This work was supported by a Genentech Predoctoral Fellowship (Z.L.), National Institutes of Health grants (DK092312 and DK106358 to S.W.; GM118167 to O.D.W.) and an American Heart Association Established Investigator Award (to O.D.W.). Deposited in PMC for release after 12 months.

Supplementary information

Supplementary information available online at
http://dev.biologists.org/lookup/doi/10.1242/dev.163535.supplemental

References

Amat, F., Lemon, W., Mossing, D. P., McDole, K., Wan, Y., Branson, K., Myers, E. W. and Keller, P. J. (2014). Fast, accurate reconstruction of cell lineages from large-scale fluorescence microscopy data. *Nat. Methods* **11**, 951-958.

Aoki, T. O., David, N. B., Minchiotti, G., Saint-Etienne, L., Dickmeis, T., Persico, G. M., Strähle, U., Mourrain, P. and Rosa, F. M. (2002a). Molecular integration of casanova in the Nodal signalling pathway controlling endoderm formation. *Development* **129**, 275-286.

Aoki, T. O., Mathieu, J., Saint-Etienne, L., Rebagliati, M. R., Peyriéras, N. and Rosa, F. M. (2002b). Regulation of Nodal signalling and mesendoderm formation by TARAM-A, a TGFβ-related type I receptor. *Dev. Biol.* **241**, 273-288.

Brunet, T., Bouclet, A., Ahmadi, P., Mitrossilis, D., Driquez, B., Brunet, A.-C., Henry, L., Serman, F., Béalle, G., Ménager, C. et al. (2013). Evolutionary conservation of early mesoderm specification by mechanotransduction in bilateria. *Nat. Commun.* **4**, 2821.

Burkel, B. M., von Dassow, G. and Bement, W. M. (2007). Versatile fluorescent probes for actin filaments based on the actin-binding domain of utrophin. *Cell Motil. Cytoskelet.* **64**, 822-832.

Carmany-Rampey, A. and Schier, A. F. (2001). Single-cell internalization during zebrafish gastrulation. *Curr. Biol.* **11**, 1261-1265.

Chan, T.-M., Longabaugh, W., Bolouri, H., Chen, H.-L., Tseng, W.-F., Chao, C.-H., Jang, T.-H., Lin, Y.-I., Hung, S. C., Wang, H. D. et al. (2009). Developmental gene regulatory networks in the Zebrafish embryo. *Biochim. Biophys. Acta* **1789**, 279-298.

Chen, Y. and Schier, A. F. (2001). The Zebrafish nodal signal squint functions as a morphogen. *Nature* **411**, 607-610.

Chung, W.-S. and Stainier, D. Y. R. (2008). Intra-endodermal interactions are required for pancreatic β cell induction. *Dev. Cell* **14**, 582-593.

Concha, M. L. and Adams, R. J. (1998). Oriented cell divisions and cellular morphogenesis in the Zebrafish gastrula and neurula: a time-lapse analysis. *Development* **125**, 983-994.

D'Amico, L. A. and Cooper, M. S. (1997). Spatially distinct domains of cell behavior in the Zebrafish organizer region. *Biochem. Cell Biol.* **75**, 563-577.

David, N. B. and Rosa, F. M. (2001). Cell autonomous commitment to an endodermal fate and behaviour by activation of Nodal signalling. *Development* **128**, 3937-3947.

Dickmeis, T., Mourrain, P., Saint-Etienne, L., Fischer, N., Aanstad, P., Clark, M., Strähle, U. and Rosa, F. (2001). A crucial component of the endoderm formation pathway, CASANOVA, is encoded by a novel Sox-related gene. *Genes Dev.* **15**, 1487-1492.

Dormann, D., Vasiev, B. and Weijer, C. J. (2000). The control of chemotactic cell movement during dictyostelium morphogenesis. *Philos. Trans. R. Soc. Lond. B Biol. Sci.* **355**, 983-991.

Dougan, S. T., Warga, R. M., Kane, D. A., Schier, A. F. and Talbot, W. S. (2003). The role of the Zebrafish Nodal-related genes Squint and Cyclops in patterning of mesendoderm. *Development* **130**, 1837-1851.

Dubrulle, J., Jordan, B. M., Akhmetova, L., Farrell, J. A., Kim, S.-H., Solnica-Krezel, L. and Schier, A. F. (2015). Response to nodal morphogen gradient is determined by the kinetics of target gene induction. *eLife* **4**, e05042.

Erter, C. E., Solnica-Krezel, L. and Wright, C. V. E. (1998). Zebrafish nodal-related 2Encodes an early mesendodermal inducer signaling from the extraembryonic yolk syncytial layer. *Dev. Biol.* **204**, 361-372.

Feldman, B. and Stemple, D. L. (2001). Morpholino phenocopies of Sqt, Oep, and Ntl mutations. *Genesis* **30**, 175-177.

Feldman, B., Gates, M. A., Egan, E. S., Dougan, S. T., Rennebeck, G., Sirotkin, H. I., Schier, A. F. and Talbot, W. S. (1998). Zebrafish organizer development and germ-layer formation require nodal-related signals. *Nature* **395**, 181-185.

Giger, F. A. and David, N. B. (2017). Endodermal germ-layer formation through active actin-driven migration triggered by N-cadherin. *Proc. Natl Acad. Sci. USA* **114**, 10143-10148.

Gritsman, K., Zhang, J., Cheng, S., Heckscher, E., Talbot, W. S. and Schier, A. F. (1999). The EGF-CFC protein one-eyed pinhead is essential for Nodal signaling. *Cell* **97**, 121-132.

Hagos, E. G. and Dougan, S. T. (2007). Time-dependent patterning of the mesoderm and endoderm by nodal signals in Zebrafish. *BMC Dev. Biol.* **7**, 22.

Hashimoto, H., Itoh, M., Yamanaka, Y., Yamashita, S., Shimizu, T., Solnica-Krezel, L., Hibi, M. and Hirano, T. (2000). Zebrafish Dkk1 functions in forebrain specification and axial mesendoderm formation. *Dev. Biol.* **217**, 138-152.

Ho, R. K. (1992). Cell movements and cell fate during zebrafish gastrulation. *Dev. Suppl.*, 65-73.

Jia, S., Ren, Z., Li, X., Zheng, Y. and Meng, A. (2008). smad2 and smad3 are required for mesendoderm induction by transforming growth factor-β/nodal signals in zebrafish. *J. Biol. Chem.* **283**, 2418-2426.

Jing, X., Zhou, S., Wang, W. and Chen, Y. (2006). Mechanisms underlying long- and short-range Nodal signaling in zebrafish. *Mech. Dev.* **123**, 388-394.

Karlen, S. and Rebagliati, M. (2001). A morpholino phenocopy of the cyclops mutation. *Genesis* **30**, 126-128.

Keller, P. J., Schmidt, A. D., Wittbrodt, J. and Stelzer, E. H. K. (2008). Reconstruction of zebrafish early embryonic development by scanned light sheet microscopy. *Science* **322**, 1065-1069.

Kikuchi, Y., Agathon, A., Alexander, J., Thisse, C., Waldron, S., Yelon, D., Thisse, B. and Stainier, D. Y. R. (2001). Casanova encodes a novel sox-related protein necessary and sufficient for early endoderm formation in zebrafish. *Genes Dev.* **15**, 1493-1505.

Kimmel, C. B. and Warga, R. M. (1987). Cell lineages generating axial muscle in the zebrafish embryo. *Nature* **327**, 234.

Kimmel, C. B., Ballard, W. W., Kimmel, S. R., Ullmann, B. and Schilling, T. F. (1995). Stages of embryonic development of the zebrafish. *Dev. Dyn.* **203**, 253-310.

Knopf, F., Hammond, C., Chekuru, A., Kurth, T., Hans, S., Weber, C. W., Mahatma, G., Fisher, S., Brand, M., Schulte-Merker, S. et al. (2011). Bone regenerates via dedifferentiation of osteoblasts in the zebrafish fin. *Dev. Cell* **20**, 713-724.

Krens, S. F. G., Veldhuis, J. H., Barone, V., Čapek, D., Maître, J.-L., Brodland, G. W. and Heisenberg, C.-P. (2017). Interstitial fluid osmolarity modulates the action of differential tissue surface tension in progenitor cell segregation during gastrulation. *Development* **144**: 1798-1806.

Krieg, M., Arboleda-Estudillo, Y., Puech, P.-H., Käfer, J., Graner, F., Müller, D. J. and Heisenberg, C.-P. (2008). Tensile forces govern germ-layer organization in zebrafish. *Nat. Cell Biol.* **10**, 429-436.
Maître, J.-L., Berthoumieux, H., Krens, S. F. G., Salbreux, G., Julicher, F., Paluch, E. and Heisenberg, C.-P. (2012). Adhesion functions in cell sorting by mechanically coupling the cortices of adhering cells. *Science* **338**, 253-256.
Mizoguchi, T., Verkade, H., Heath, J. K., Kuroiwa, A. and Kikuchi, Y. (2008). Sdf1/Cxcr4 signaling controls the dorsal migration of endodermal cells during zebrafish gastrulation. *Development* **135**, 2521-2529.
Montero, J.-A., Carvalho, L., Wilsch-Bräuninger, M., Kilian, B., Mustafa, C. and Heisenberg, C.-P. (2005). Shield formation at the onset of zebrafish gastrulation. *Development* **132**, 1187-1198.
Nair, S. and Schilling, T. F. (2008). Chemokine signaling controls endodermal migration during zebrafish gastrulation. *Science* **322**, 89-92.
Nance, J. and Priess, J. R. (2002). Cell polarity and gastrulation in *C. Elegans*. *Development* **129**, 387-397.
Paskaradevan, S. and Scott, I. C. (2012). The Aplnr GPCR regulates myocardial progenitor development via a novel cell-non-autonomous, Gαi/o protein-independent pathway. *Biol. Open* **1**, 275-285.
Pauli, A., Norris, M. L., Valen, E., Chew, G.-L., Gagnon, J. A., Zimmerman, S., Mitchell, A., Ma, J., Dubrulle, J., Reyon, D. et al. (2014). Toddler: an embryonic signal that promotes cell movement via apelin receptors. *Science* **343**, 1248636.
Peyriéras, N., Strähle, U. and Rosa, F. (1998). Conversion of zebrafish blastomeres to an endodermal fate by TGF-β-related signalling. *Curr. Biol.* **8**, 783-788.
Pézeron, G., Mourrain, P., Courty, S., Ghislain, J., Becker, T., Rosa, F. and David, N. (2008). Live analysis of endodermal layer formation identifies random walk as a novel gastrulation movement. *Curr. Biol.* **18**, 276-281.
Piccolo, S. (2013). Developmental biology: mechanics in the embryo. *Nature* **504**, 223-225.
Pogoda, H.-M., Solnica-Krezel, L., Driever, W. and Meyer, D. (2000). The zebrafish forkhead transcription factor FoxH1/Fast1 is a modulator of Nodal signaling required for organizer formation. *Curr. Biol.* **10**, 1041-1049.
Renucci, A., Lemarchandel, V. and Rosa, F. (1996). An activated form of type I serine/threonine kinase receptor TARAM-A reveals a specific signalling pathway involved in fish head organiser formation. *Development* **122**, 3735-3743.
Sakaguchi, T., Kuroiwa, A. and Takeda, H. (2001). A novel Sox gene, 226D7, acts downstream of Nodal signaling to specify endoderm precursors in zebrafish. *Mech. Dev.* **107**, 25-38.
Schier, A. F. and Shen, M. M. (2000). Nodal signalling in vertebrate development. *Nature* **403**, 385-389.
Scott, I. C., Masri, B., D'Amico, L. A., Jin, S.-W., Jungblut, B., Wehman, A. M., Baier, H., Audigier, Y. and Stainier, D. Y. R. (2007). The G protein-coupled receptor Agtrl1b regulates early development of myocardial progenitors. *Dev. Cell* **12**, 403-413.
Shivdasani, R. A. (2002). Molecular regulation of vertebrate early endoderm development. *Dev. Biol.* **249**, 191-203.
Steinberg, M. S. (1962). On the mechanism of tissue reconstruction by dissociated cells, I. population kinetics, differential adhessiveness, and the absence of directed migration. *Proc. Natl. Acad. Sci. USA* **48**, 1577-1582.
Stern, C. D. (2004). *Gastrulation: From Cells to Embryo*. Cold Spring Harbor, New York, USA: Cold Spring Harbor Laboratory Press.
Takaku, Y., Hariyama, T. and Fujisawa, T. (2005). Motility of endodermal epithelial cells plays a major role in reorganizing the two epithelial layers in hydra. *Mech. Dev.* **122**, 109-122.
Trinkaus, J. P. (1984). *Cells into Organs (the Forces That Shape the Embryo)*, Vol. 8, p. 422. Upper Saddle River, New Jersey, USA: Prentice-Hall:
Voiculescu, O., Bodenstein, L., Lau, I.-J. and Stern, C. D. (2014). Local cell interactions and self-amplifying individual cell ingression drive amniote gastrulation. *eLife* **3**, e01817.
Warga, R. M. and Kane, D. A. (2003). One-eyed pinhead regulates cell motility independent of squint/cyclops signaling. *Dev. Biol.* **261**, 391-411.
Warga, R. M. and Kimmel, C. B. (1990). Cell movements during epiboly and gastrulation in zebrafish. *Development* **108**, 569-580.
Weng, W. and Stemple, D. L. (2003). Nodal signaling and vertebrate germ layer formation. *Birth Defects Res. C Embryo Today* **69**, 325-332.
Wolpert, L. (1992). Gastrulation and the evolution of development. *Dev. Suppl.*, 7-13.
Woo, S., Housley, M. P., Weiner, O. D. and Stainier, D. Y. R. (2012). Nodal signaling regulates endodermal cell motility and actin dynamics via Rac1 and Prex1. *J. Cell Biol.* **198**, 941-952.
Xiong, F., Tentner, A. R., Huang, P., Gelas, A., Mosaliganti, K. R., Souhait, L., Rannou, N., Swinburne, I. A., Obholzer, N. D., Cowgill, P. D. et al. (2013). Specified neural progenitors sort to form sharp domains after noisy Shh signaling. *Cell* **153**, 550-561.

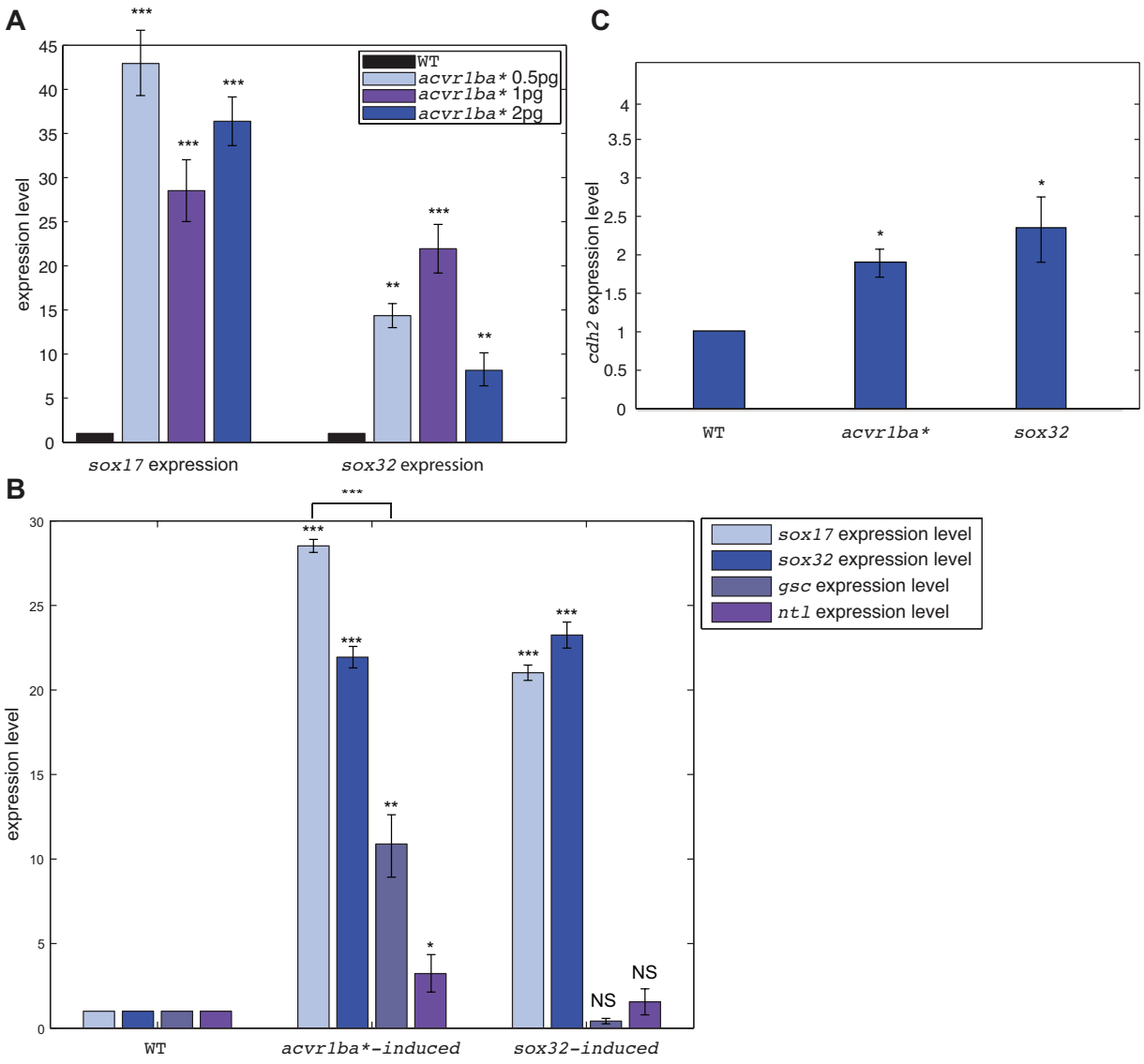

Figure S1: ***acvr1ba**** **induces expression of *sox17* and *sox32*. Related to Figure 1.**

(A) Expression of *sox17* and *sox32* endodermal markers was measured by real-time quantitative PCR. Constitutive activation of the Nodal pathway by expression of *acvr1ba** upregulated *sox17* and *sox32* expression (normalized to uninjected controls). **p<0.01, ***p<0.001.

(B) Expression of *sox17*, *sox32*, *gsc* and *ntl* was measured by real-time quantitative PCR in *acvr1ba**-expressing cells and *sox32*-expressing cells in wildtype background. Both acvrb1a* and sox32 more potently induce endodermal markers (*sox17* and *sox32*) than mesodermal markers (*gsc* and *ntl*). *p<0.05, **p<0.01, ***p<0.001, NS, not significant.

(C) Expression of *cdh2* at 6hpf was measured by real-time quantitative PCR. Both *acvr1ba** and *sox32*-induced endodermal cells have elevated expression comparing to wild type uninjected controls. *p<0.05.

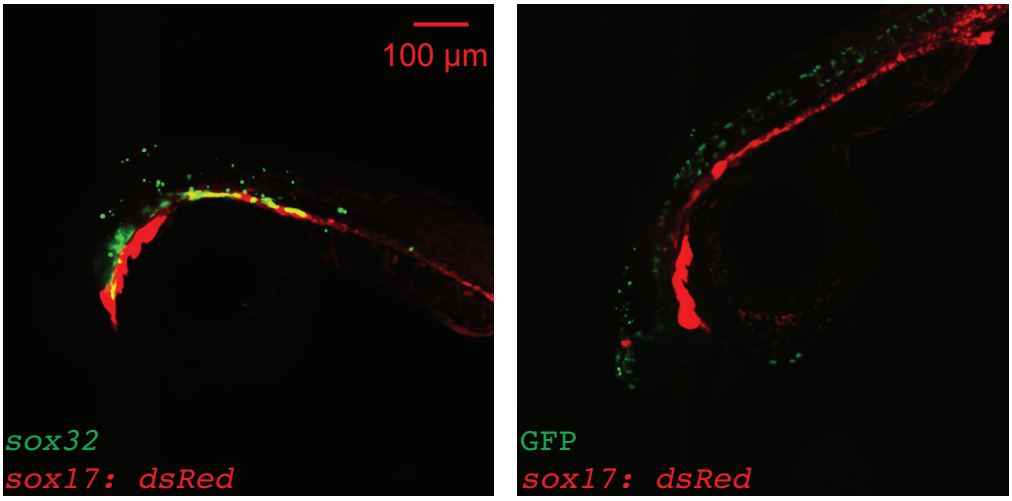

Figure S2: *sox32*-expressing cells preferentially segregate to endoderm-derived tissues when placed near the dorsal margin. Related to Figure 2.

Representative images showing distribution of *sox32*-overexpressing cells or GFP-expressing cells that were transplanted to the margin of wild-type host embryos. At 21-somite stage, transplanted *sox32*-overexpressing cells primarily localized to endodermal tissues while GFP-expressing cells localized to mesodermal tissues.

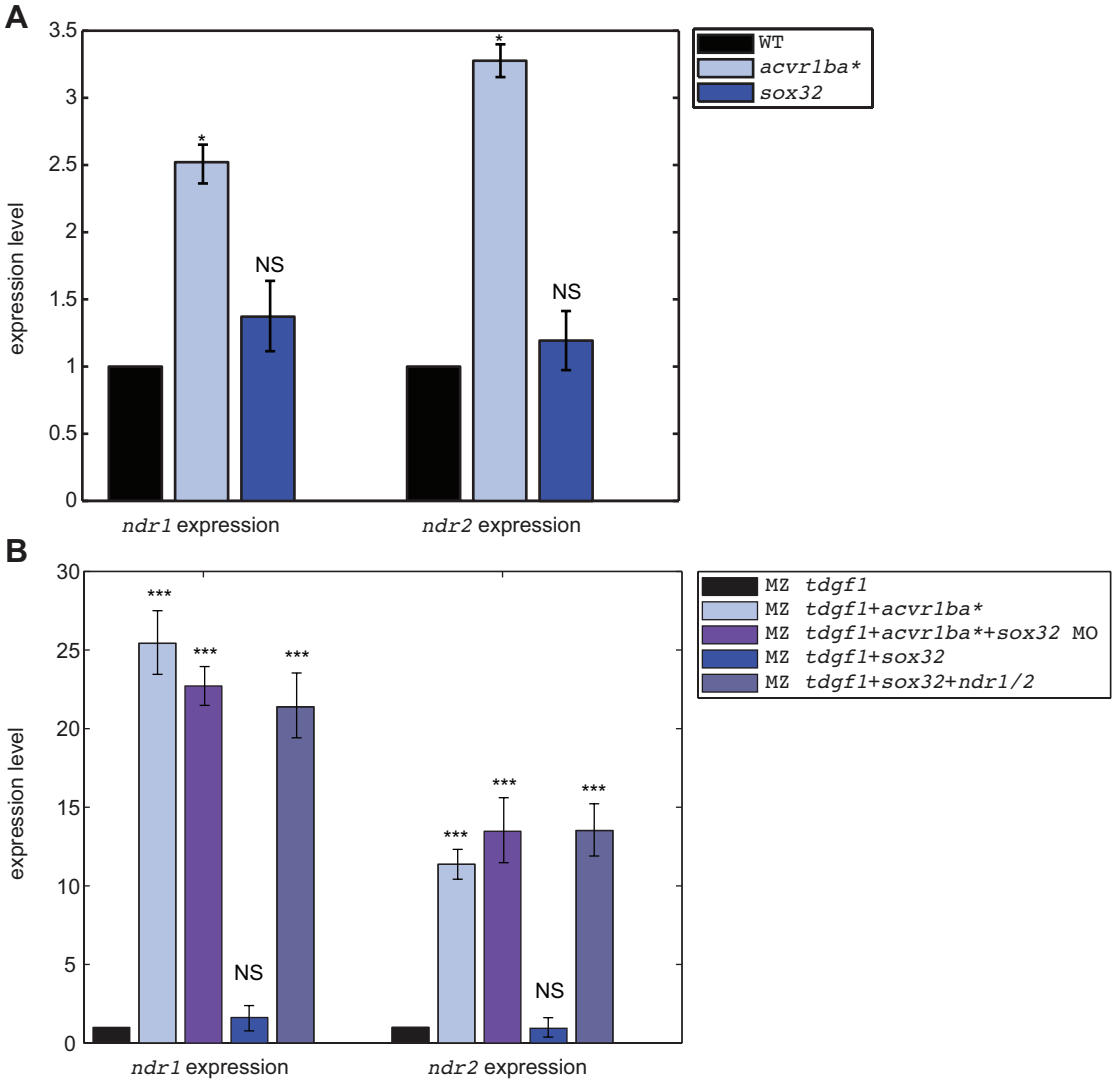

Figure S3: ***ndr1/2* is upregulated by *acvr1ba**, and *sox32* is neither necessary or sufficient for this upregulation. Related to Figure 2.**

(A) *ndr1/2* expression in *acvr1ba**-expressing cells and *sox32*-overexpressing cells in wildtype background measured by real-time quantitative PCR. *p<0.05, NS, not significant.

(B) *ndr1/2* expression under all experimental conditions in MZ *tdgf1* background, which removes the confounding effects of maternally deposited Ndr1/2 on driving nodal signaling. ***p<0.001, NS, not significant.

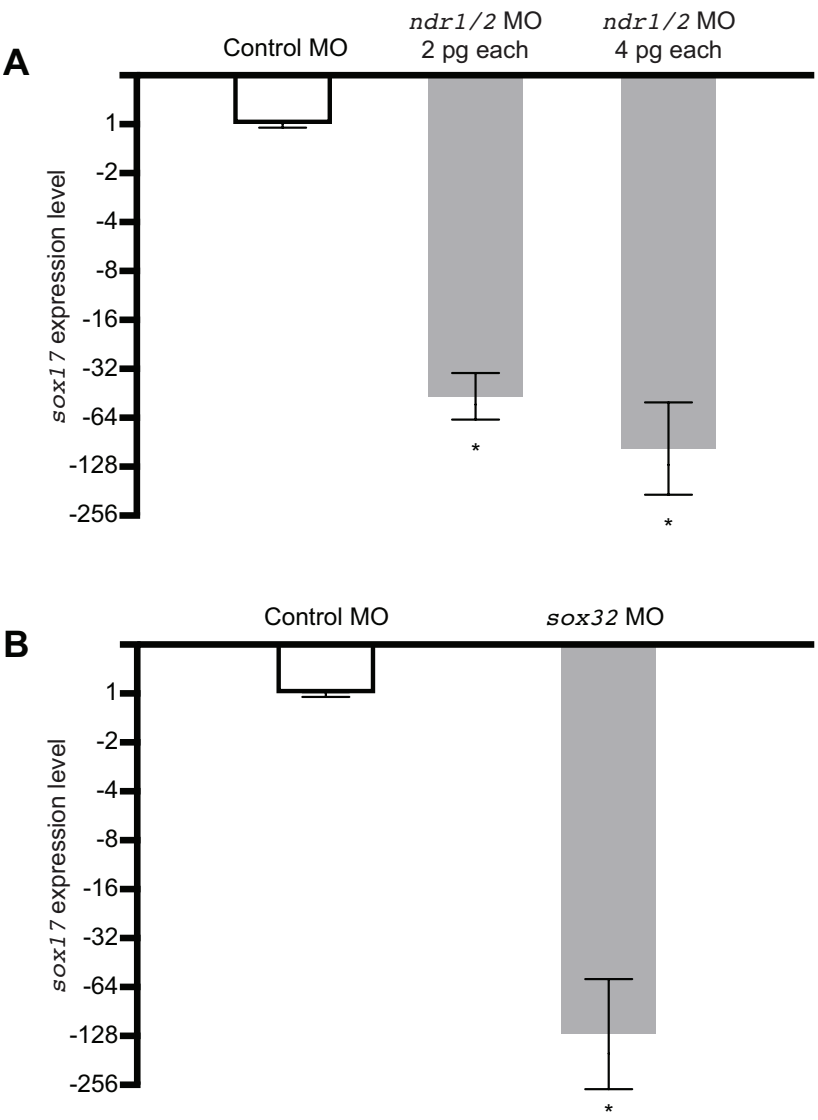

Figure S4: Validation of *ndr1*, *ndr2* and *sox32* morpholinos. Related to Figure 2.

(A) Validation of *ndr1/2* knockdown. Embryos were injected at the 1-cell stage with standard control (Gene Tools) or *ndr1* and *ndr2* MO. Total RNA was collected at 70% epiboly (7 hpf), and *sox17* expression was quantified by qPCR. ndr1/2 knockdown reduced *sox17* expression by 50-fold when 2pg each was injected and 80-fold when 4pg each was injected. Data represents averages of 3 biological replicates. Error bars, S.E.M. *p=0.01.

(B) Validation of *sox32* knockdown. Embryos were injected at the 1-cell stage with 2ng of standard control (Gene Tools) or *sox32* MO. Total RNA was collected at 70% epiboly (7 hpf), and *sox17* expression was quantified by qPCR. *sox32* knockdown reduced *sox17* expression by 125-fold. Data represents averages of 3 biological replicates. Error bars, S.E.M. *p=0.01.

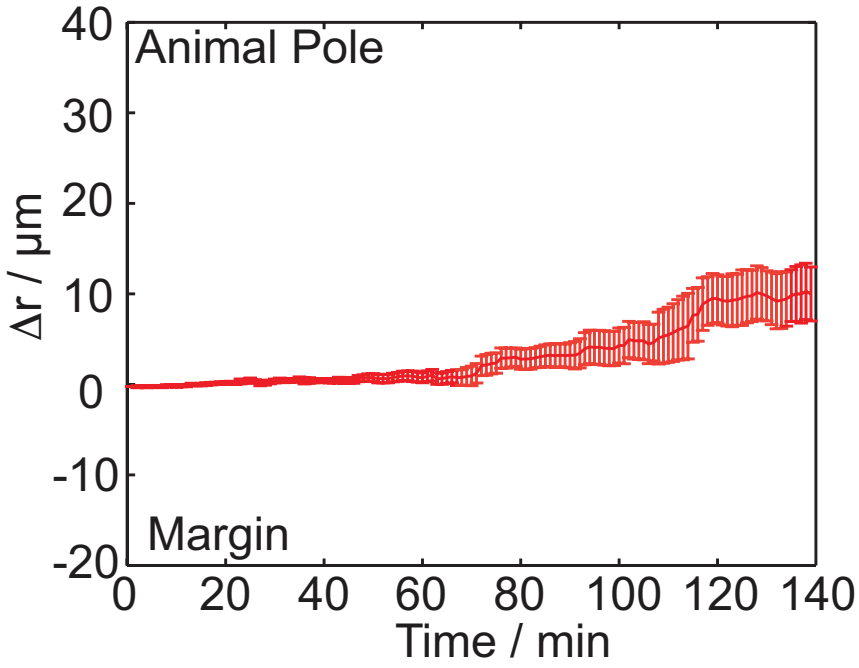

Figure S5: Single-cell tracking analysis of ingression of *acvr1ba-expressing cells with *sox32* MO. Related to Figure 2.**

Average relative distance with standard error plotted against time. Relative distance was calculated as in Fig. 2I. Unlike cells expressing *acvr1ba** only, cells also containing *sox32* MO move toward the surface of the embryo with their ectodermal neighbors.

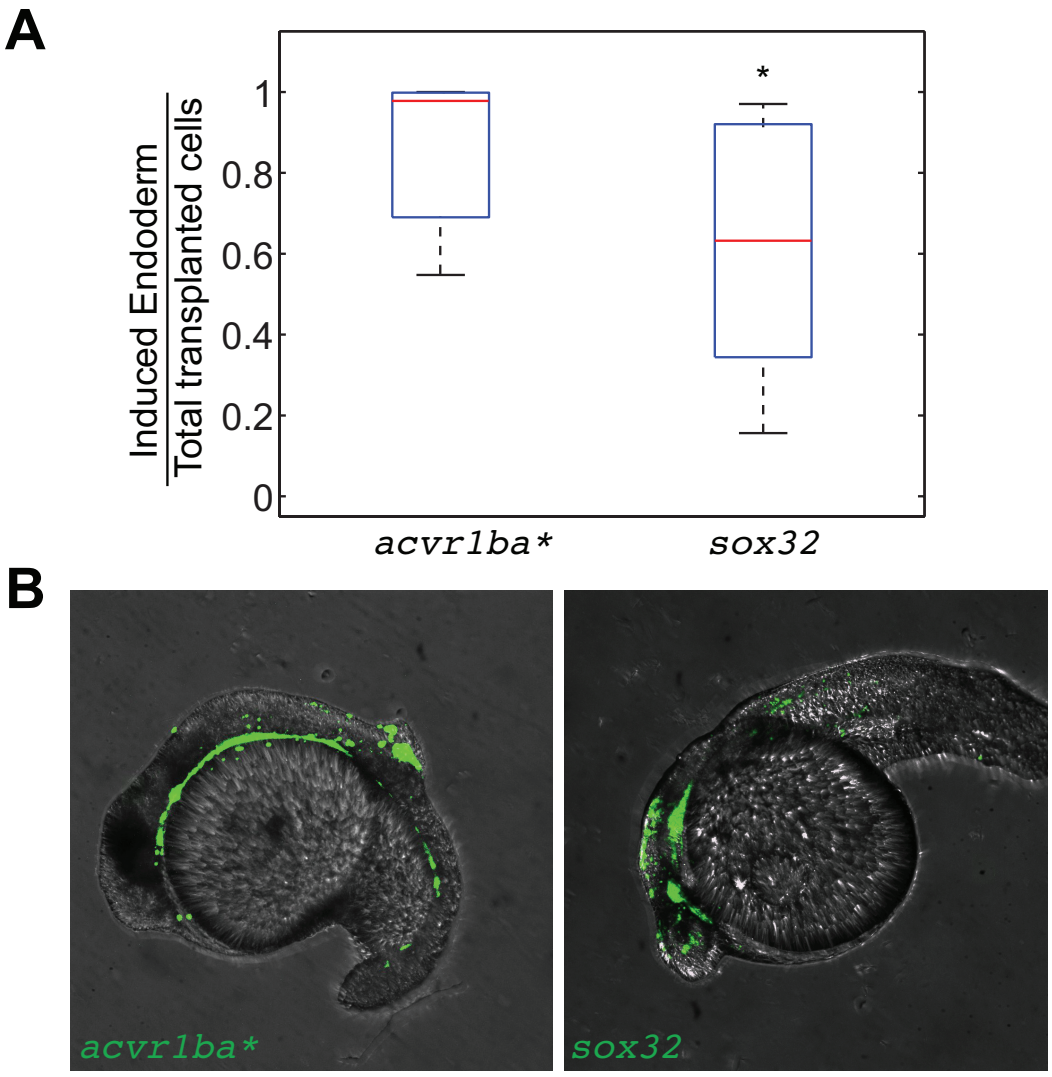

Figure S6: Induced endodermal cells internalize following transplantation to the margin.
(A) Boxplot quantification of endoderm contribution of transplanted cells at 18 hpf. Data is shown as mean ± SEM of independent transplantation experiments with 14 embryos per condition. Student's t-test was performed. * $p<0.05$.
(B) Representative image showing distribution of transplanted cells depicted in (A) at 18 hpf. *acvr1ba**-expressing cells localized to the endoderm-derived tissue (green). Cells overexpressing *sox32* localize to both endoderm and ectoderm-derived tissue. Lateral view, anterior to the left.

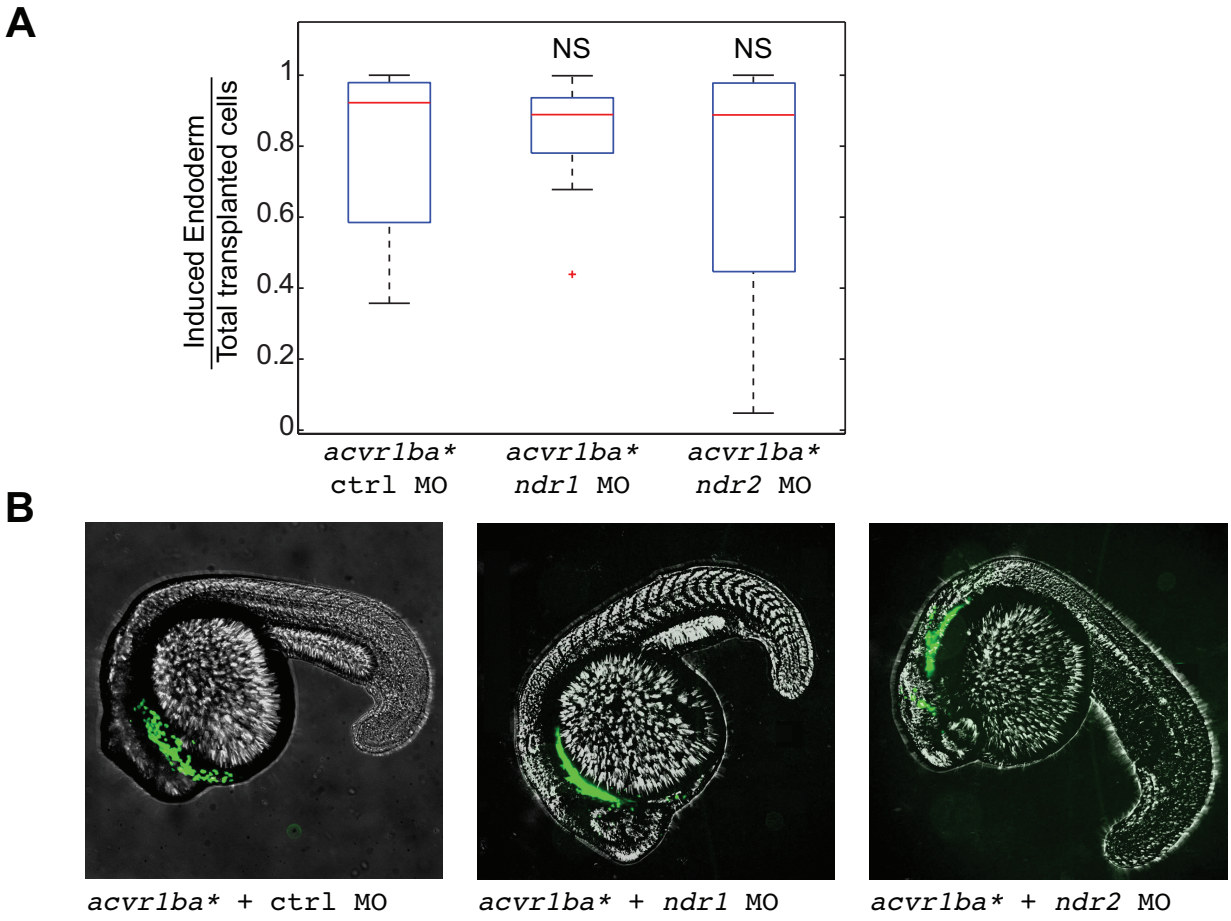

Figure S7: Ndr1 and Ndr2 act redundantly to support the ability of *acvr1ba cells to internalize.**

(A) Boxplot quantification of endoderm contribution of transplanted cells at 20 hpf. Data is shown as mean ± SEM of independent transplantation experiments with 16 embryos per condition. Student's t-test was performed. NS, not significant.

(B) Representative image showing distribution of transplanted cells depicted in (A) at 18 hpf. *acvr1ba**-expressing cells localized to the endoderm-derived tissue (green)in all three conditions, in contrast to the block of internalization when both Ndr1 and Ndr2 MO are combined in acvr1ba* cells (**Fig. 2H**). Lateral view, anterior to the left.

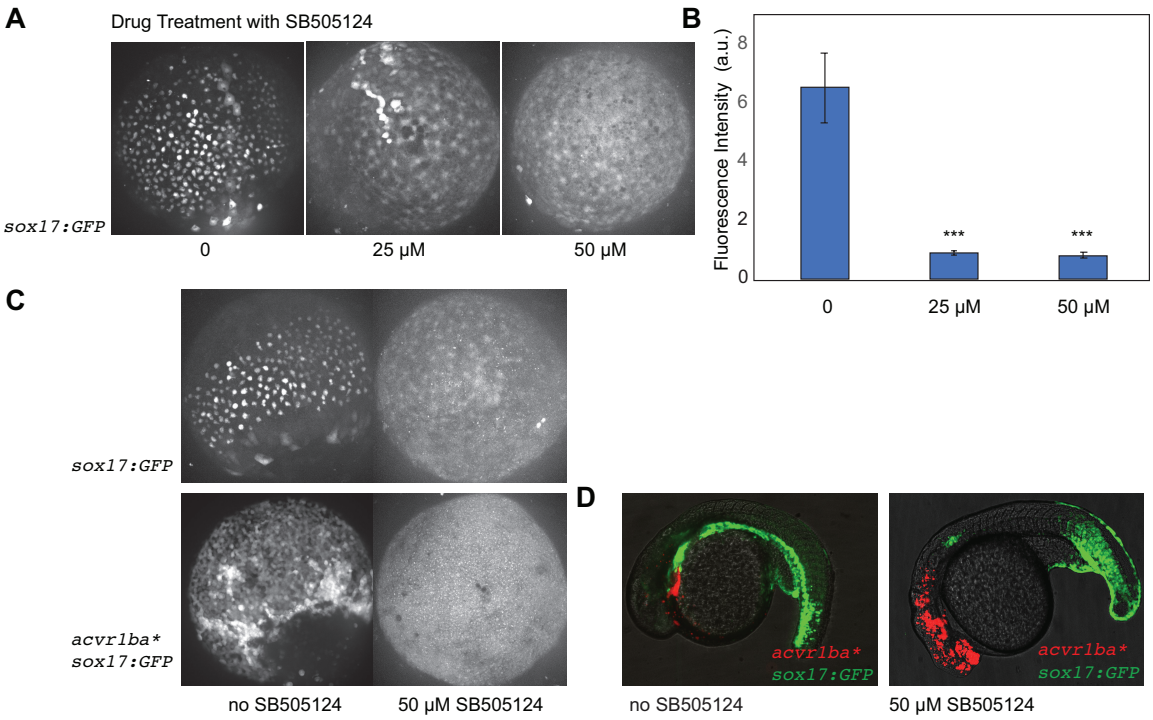

Figure S8: Nodal signaling inhibitor SB505124 blocks *acvr1ba-expressing cells from sorting.**

(A) Representative images of *sox17:GFP* expression under 0, 25 μM or 50 μM SB505124. Drug treatment began at 6 hpf, images were taken at 10 hpf. Animal pole view.

(B) Quantification of *sox17:GFP* fluorescence intensity under 0, 25 μM or 50 μM SB505124. *** p<0.001. n=3.

(C) *sox17:GFP* expression for embryos with or without injection of acvr1ba* and under no drug treatment or treated 50 μM drug SB505124 treatment.

(D) Transplant of *acvr1ba**-expressing cells into *sox17:GFP* background under DMSO control and 50 μM drug SB505124 treatment at 18hfp.

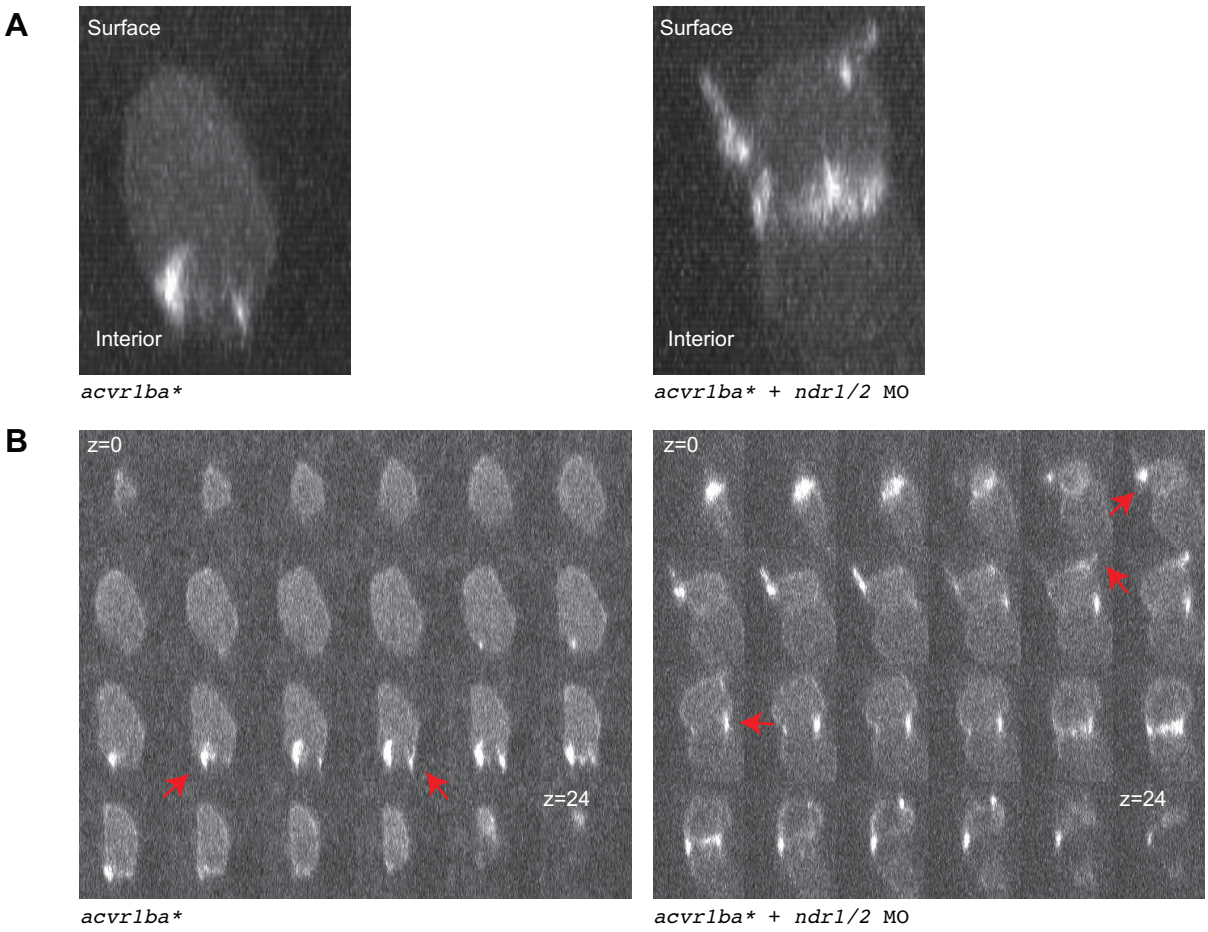

Figure S9: Blocking autocrine production of *ndr1/2* interferes with polarity of actin-based protrusions in *acvr1ba cells. Related to Figure 5.**

(A) Maximum? Z projection of individual transplanted cells injected with either *acvr1ba** alone or *acvr1ba** with *ndr1/2* MOs.

(B) Montage of Z stack of cells shown in (A). Red arrows indicate actin enrichment. Numbers indicate μm?

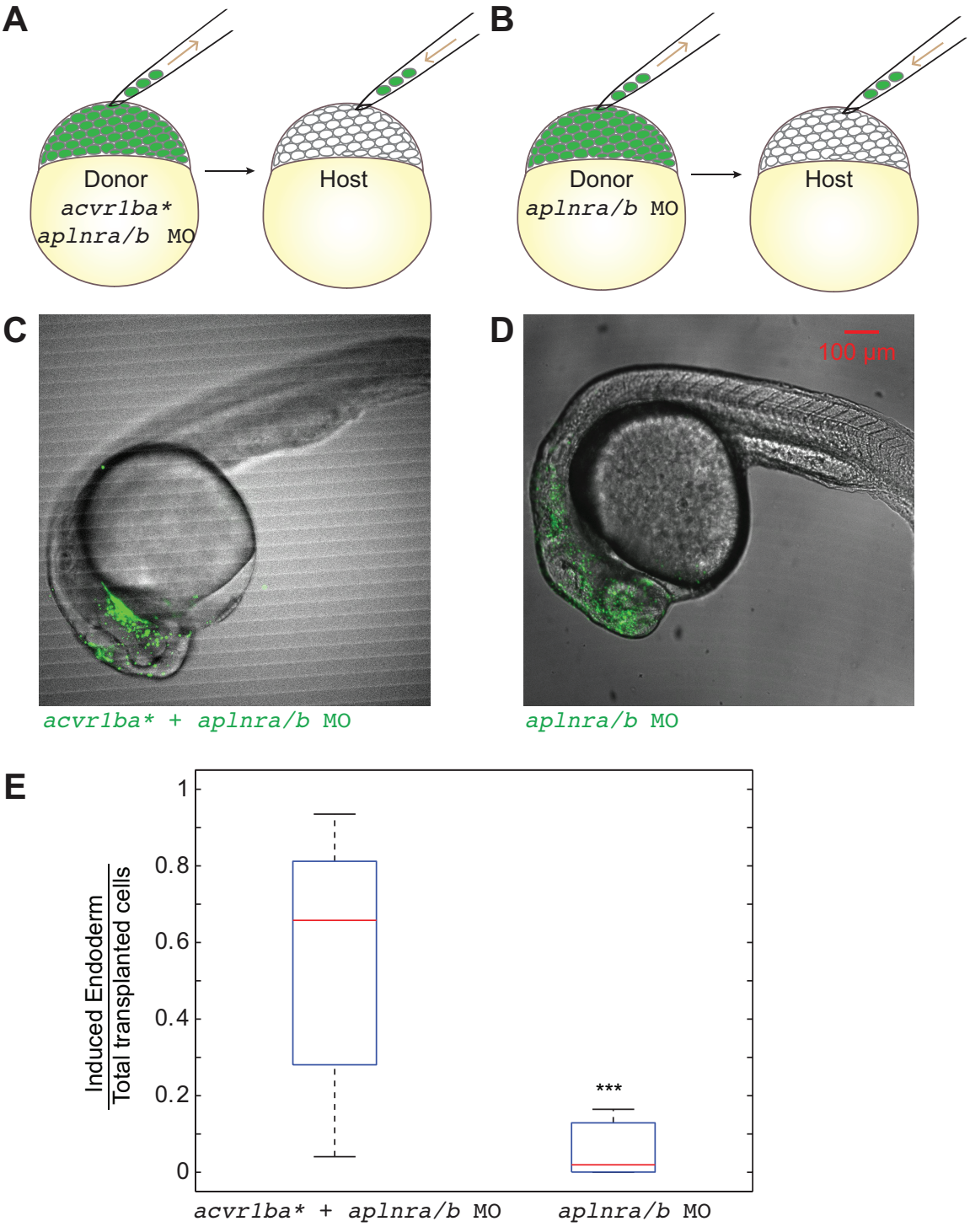

Figure S10: **Apelin receptor signaling is not essential for ectopic endoderm ingression.** **(A-B)** Schematic diagrams depicting single donor transplant assay to test the role of apelin receptor signaling. (A) *acvr1ba**-expressing cells with *aplnra* and *aplnrb* MOs were transplanted

to the animal pole of a wild-type host embryo. (B) Cells with *aplnra* and *aplnrb* MOs alone were transplanted to the animal pole of a wild-type host embryo.
(C-D) Representative images showing distribution of induced endodermal cells in a wild-type host. Donor cells in (A) (green) mainly localized to endoderm-derived tissue (C), while donor cells in (B) mainly localized to ectoderm-derived tissue (D). Lateral view, anterior to the right.
(E) Boxplot quantification of endoderm contribution at 21 hpf of transplanted cells depicted in (A-B). *acvr1ba**-expressing cells with *aplnra* and *aplnrb* MOs contributed to endoderm significantly more than cells with *aplnra* and *aplnrb* MOs alone. Data is shown as mean ± SEM of 3 independent transplantation experiments with 18 embryos per condition. Student's t-test was performed. *** $p<0.001$.

Table S1. List of Oligonucleotides

Oligonucleotide Name	Sequence
ef1a_forward	5′-CAAGAAGAGTAGTACCGCTAGCAT-3′
ef1a_reverse	5′-CACGGTGACAACATGCTGGAG-3′
sox17_forward	5'-CACAATGCGGAGCTGAGTAA-3'
sox17_reverse	5'-GCCTCCTCAACGAATGGAC-3'
sox32_forward	5'-CGGACCTGGAGAACACTGAC-3'
sox32_reverse	5'-GCATGTACGGACGCTTATCTG-3'
cdh2_forward	5'-CATCCCGGAGACATAGGAGA-3'
cdh2_reverse	5'-GCCCTCGTAGTCAAACACCA-3'
Oep5	5'-GAGATGGAGATGTTCTAATG-3'
Oep3m	5'-GAACAGTTGACTCGTCAC-3'
Oep3w	5'-GAACAGTTGACTCGTCAT-3'
Sox32 MO	5'-GCATCCGGTCGACATACATGCTGTT-3'
Sqt MO	5'-ATGTCAAATCAAGGTAATAATCCAC-3'
Cyc MO	5'-GCGACTCCCGAGCGTGTGCATGATG-3'
Aplnr a MO	5'-CGGTGTATTCCGGCGTTGGCTCCAT-3'
Aplnr b MO	5'-CAGAGAAGTTGTTTGTCATGTGCTC-3'
Control MO	5'-CCTCTTAACCTCAGTTACAATTTATA-3'

Table S2. Key Resource Table

Reagent or Resource	Source	Identifier
Chemicals, Peptides, and Recombinant Proteins		
Dextran, Alexa Fluor™ 647	Invitrogen	Cat#D22914

Dextran, Tetramethylrhodamine	Invitrogen	Cat#D1868
Dextran, Fluorescein	Invitrogen	Cat#D1821
Dextran, Alexa Fluor™ 680	Invitrogen	Cat#D34680
Histone H1 From Calf Thymus, Alexa Fluor™ 488 Conjugate	Invitrogen	Cat#H13188
Critical Commercial Assays		
mMESSAGE mMACHINE SP6 Transcription Kit	Ambion	Cat#AM1340
SuperScript VILO cDNA Synthesis Kit	Invitrogen	Cat#11754050
SYBR green PCR master mix	Applied Biosciences	Cat#4309155
Experimental Models: Organisms/Strains		
Zebrafish: AB/TL	This study	ZFIN: ZDB-GENO-960809-7
Zebrafish: EKW	This study	ZFIN: ZDB-GENO-031202-1
Zebrafish: Tg(sox17:GFP)	This study	ZFIN: ZDB-GENO-061228-1
Zebrafish: Tg(sox17:DsRed)	This study	ZFIN: ZDB-GENO-080812-1
Zebrafish: Tg(h2afva:h2afva-mCherry)	This study	ZFIN: ZDB-GENO-100923-1
Zebrafish: Tg(ubb:GFP-Smad2)	This study	N/A

Zebrafish: *tdgf1*$^{tz57/+}$	Lilianna Solnica-Krezel lab	ZFIN: ZDB-GENO-080708-1
Zebrafish: *tdgf1*$^{tz57/tz57}$	This study	ZFIN: ZDB-GENO-980202-989
Oligonucleotides		
List of oligonucleotides	See Table S1	N/A
Recombinant DNA		
pCS2-acbr1ba*	This study	N/A
pCS2-acbr1ba*-p2a-tBFP	This study	N/A
pCS2-sox32	This study	N/A
pCS2-sox32-p2a-tBFP	This study	N/A
pCS2-ndr1	This study	N/A
pCS2-ndr1-GFP	This study	N/A
pCS2-ndr2	This study	N/A
pCS2-ndr2-tBFP	This study	N/A
pCS2-GFP-UTRN	This study	N/A
pCS2-GFP	This study	N/A
pCS2-h2a-mCherry	This study	N/A
pCS2-tdgf1	This study	N/A
pmTol2-ef1a:Venus-Smad2	Steve Harvey	N/A
Software and Algorithms		

Fiji	NIH	https://fiji.sc
Matlab2013a	MathWorks Inc.	http://mathworks.com
TGMM	Philipp Keller lab	https://www.janelia.org/lab/keller-lab/software/fast-accurate-reconstruction-cell-lineages-large-scale-fluorescence

Contact for Reagent and Resource Sharing

Further information and requests for resources and reagents should be directed to Orion Weiner (orion.weiner@ucsf.edu).

Movie S1: *acvr1ba**-induced endodermal cells ingress into the inner layer when transplanted to the animal pole. Related to Figure 1. Frames were acquired every 5 min for 195 min. Playback is 7 frames/s.

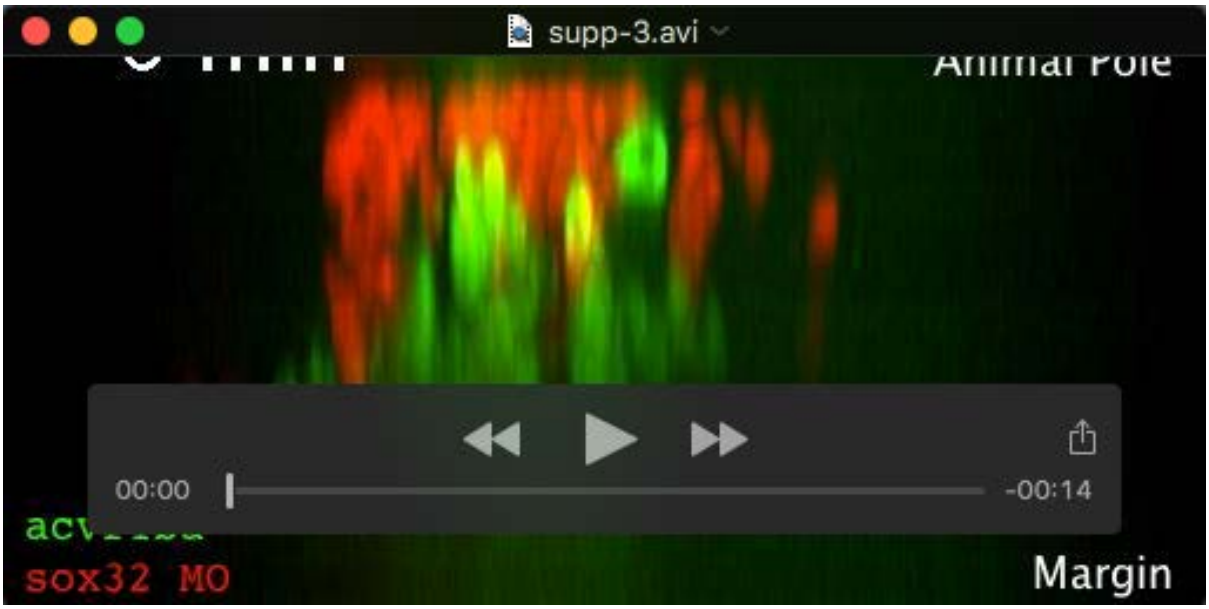

Movie S2: *acvr1ba**-induced endodermal cells and *sox32* MO induced ectodermal cells segregate into two separate layers. *sox32* MO-injected donor cells (red) remain on the outer layer of the embryo, while *acvr1ba**-injected donor cells (green) migrate into the inner layer of the embryo. Related to Figure 1. Frames were acquired every 3 min for 288 min. Playback is 7 frames/s.